Article

Synthetic, Mechanistic, and Computational Investigations of Nitrile-Alkyne Cross-Metathesis

Andrea M. Geyer, Eric S. Wiedner, J. Brannon Gary, Robyn L. Gdula, Nicola C. Kuhlmann, Marc J. A. Johnson, Barry D. Dunietz, and Jeff W. Kampf

J. Am. Chem. Soc., **2008**, 130 (28), 8984-8999 • DOI: 10.1021/ja800020w • Publication Date (Web): 20 June 2008

J|A|C|S
ARTICLES

Published on Web 06/20/2008

Synthetic, Mechanistic, and Computational Investigations of Nitrile-Alkyne Cross-Metathesis

Andrea M. Geyer, Eric S. Wiedner, J. Brannon Gary, Robyn L. Gdula, Nicola C. Kuhlmann, Marc J. A. Johnson,* Barry D. Dunietz, and Jeff W. Kampf

Department of Chemistry, University of Michigan, 930 North University Avenue, Ann Arbor, Michigan 48109-1055

Received January 2, 2008; E-mail: mjaj@umich.edu

Abstract: The terminal nitride complexes $NW(OC(CF_3)_2Me)_3(DME)$ (**1**-DME), $[Li(DME)_2][NW(OC(CF_3)_2Me)_4]$ (**2**), and $[NW(OCMe_2CF_3)_3]_3$ (**3**) were prepared in good yield by salt elimination from $[NWCl_3]_4$. X-ray structures revealed that **1**-DME and **2** are monomeric in the solid state. All three complexes catalyze the cross-metathesis of 3-hexyne with assorted nitriles to form propionitrile and the corresponding alkyne. Propylidyne and substituted benzylidyne complexes $RCW(OC(CF_3)_2Me)_3$ were isolated in good yield upon reaction of **1**-DME with 3-hexyne or 1-aryl-1-butyne. The corresponding reactions failed for **3**. Instead, $EtCW(OC(CF_3)Me_2)_3$ (**6**) was prepared via the reaction of $W_2(OC(CF_3)Me_2)_6$ with 3-hexyne at 95 °C. Benzylidyne complexes of the form $ArCW(OC(CF_3)Me_2)_3$ (Ar = aryl) then were prepared by treatment of **6** with the appropriate symmetrical alkyne ArCCAr. Three coupled cycles for the interconversion of **1**-DME with the corresponding propylidyne and benzylidyne complexes via [2 + 2] cycloaddition−cycloreversion were examined for reversibility. Stoichiometric reactions revealed that both nitrile-alkyne cross-metathesis (NACM) cycles as well as the alkyne cross-metathesis (ACM) cycle operated reversibly in this system. With catalyst **3**, depending on the aryl group used, at least one step in one of the NACM cycles was irreversible. In general, catalyst **1**-DME afforded more rapid reaction than did **3** under comparable conditions. However, **3** displayed a slightly improved tolerance of polar functional groups than did **1**-DME. For both **1**-DME and **3**, ACM is more rapid than NACM under typical conditions. Alkyne polymerization (AP) is a competing reaction with both **1**-DME and **3**. It can be suppressed but not entirely eliminated via manipulation of the catalyst concentration. As AP selectively removes 3-hexyne from the system, tandem NACM-ACM-AP can be used to prepare symmetrically substituted alkynes with good selectivity, including an arylene-ethynylene macrocycle. Alternatively, unsymmetrical alkynes of the form EtCCR (R variable) can be prepared with good selectivity via the reaction of RCN with excess 3-hexyne under conditions that suppress AP. DFT calculations support a [2 + 2] cycloaddition−cycloreversion mechanism analogous to that of alkyne metathesis. The barrier to azametalacyclobutadiene ring formation/breakup is greater than that for the corresponding metalacyclobutadiene. Two distinct high-energy azametalacyclobutadiene intermediates were found. These adopted a distorted square pyramidal geometry with significant bond localization.

Introduction

Recently, we communicated a new approach for synthesizing symmetrical alkynes via the cross-metathesis of a sacrificial alkyne (R′CCR′) with a nitrile (RCN) catalyzed by the metal-nitride complexes $N{\equiv}W(OC(CF_3)_2Me)_3(DME)$ (**1**-DME), $[Li(DME)_2][N{\equiv}W(OC(CF_3)_2Me)_4]$ (**2**), and $[N{\equiv}W(OCMe_2CF_3)_3]_3$ (**3**).[1] This effected coupling of the R′C and RC units of the nitrile and alkyne to produce RCCR′, which underwent subsequent reactions to form RCCR. Herein, we describe mechanistic variations in nitrile-alkyne cross-metathesis (NACM) as a function of the catalyst identity and choice of nitrile as revealed through synthetic and kinetic investigations. Computational analyses of NACM using density functional theory (DFT) indicate nearly isoenergetic tungsten-nitride and tungsten-alkylidyne catalyst states along with a moderate barrier to metalacycle formation and subsequent ring opening. Applications of the system to the formation of symmetrical alkynes, unsymmetrical alkynes, and an arylene-ethynylene macrocycle are also detailed.

Advances in the development of catalysts for alkyne metathesis (AM) have sparked an increased interest in the application of AM to the synthesis of a wide variety of materials.[2–5] Previously, application of alkyne metathesis was infrequent, in part because of the difficulty of synthesizing the required catalysts.[6–9] However, several alkyne metathesis precatalysts can

(1) Geyer, A. M.; Gdula, R. L.; Wiedner, E. S.; Johnson, M. J. A. *J. Am. Chem. Soc.* **2007**, *129*, 3800.

(2) Schrock, R. R.; Czekelius, C. *Adv. Synth. Catal.* **2007**, *349*, 55.
(3) Zhang, W.; Moore, J. S. *Angew. Chem., Int. Ed.* **2006**, *45*, 4416.
(4) Furstner, A. Davies, P. W. *Chem. Commun.* **2005**, 2307 and references therein.
(5) Zhang, W.; Moore, J. S. *Adv. Synth. Catal.* **2007**, *349*, 93.
(6) McCullough, L. G.; Schrock, R. R.; Dewan, J. C.; Murdzek, J. C. *J. Am. Chem. Soc.* **1985**, *107*, 5987.
(7) Freudenberger, J. H.; Schrock, R. R.; Churchill, M. R.; Rheingold, A. L.; Ziller, J. W. *Organometallics* **1984**, *3*, 1563.
(8) Listemann, M. L.; Schrock, R. R. *Organometallics* **1985**, *4*, 74.
(9) Schrock, R. R.; Clark, D. N.; Sancho, J.; Wengrovius, J. H.; Rocklage, S. M.; Pedersen, S. F. *Organometallics* **1982**, *1*, 1645.

10.1021/ja800020w CCC: $40.75

Scheme 1. NACM via Reversible Interconversion of Nitride and Alkylidyne Ligands

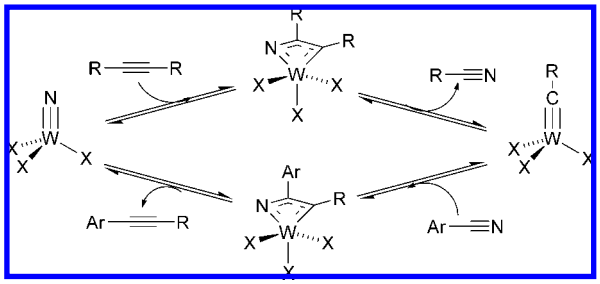

now be accessed readily through a variety of methods.[2,10–18] These precatalysts range in identity, but in general, the proposed active species is a metal-alkylidyne complex. As a result of the increased accessibility of metal-alkylidyne complexes, large macrocycles, polymers, and natural products were successfully synthesized via alkyne metathesis.[3–5,19] Unfortunately, one of the drawbacks of alkyne metathesis is the requirement for preexisting carbon−carbon triple bonds, which can be difficult to install. Therefore, an alternative method for the synthesis of alkynes that utilizes more readily accessible precursors is desired.

In general, the nitrile functionality can be incorporated into a molecule more readily than the alkyne moiety.[20,21] This spurred us to develop a method to convert a nitrile into an alkyne cleanly and efficiently. This transformation necessarily requires the ability to interconvert alkylidyne and nitride ligands. Reversibility permits productive catalysis. The proposed cycle for tungsten-catalyzed NACM is detailed in Scheme 1.

A precedent for the alkylidyne-to-nitride conversion is provided by Schrock's work with RC≡W(O-*t*-Bu)$_3$, in which N≡W(O-*t*-Bu)$_3$ is formed upon treatment with PhCN.[22] Chisholm similarly demonstrated the stoichiometric conversion of PhC≡W(OC(CF$_3$)Me$_2$)$_3$ into the trimeric nitrido complex [N≡W(OC(CF$_3$)Me$_2$)$_3$]$_3$.[23] Recently, we provided the first example of a conversion in the opposite direction: N≡Mo(OC(CF$_3$)$_2$Me)$_3$ undergoes metathesis with 3-heyxne at high temperatures to produce the corresponding propylidyne complex EtC≡Mo(OC(CF$_3$)$_2$Me)$_3$.[10] A summary of known interconversions of alkylidyne and nitride species is provided in Scheme 2.

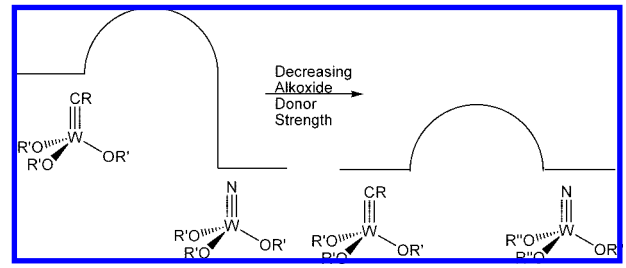

Figure 1. Impact of alkoxide on relative energies of alkylidyne and nitride complexes.

Scheme 2. Known Interconversions of Alkylidyne and Nitride Complexes

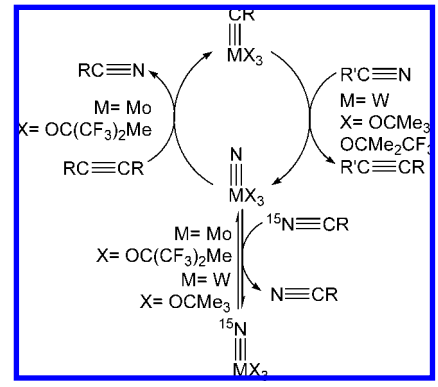

Seeking a catalyst that would permit the reversible formation of a metal-alkylidyne complex from the corresponding nitride species, we chose tungsten-alkoxides as a starting point. As a less electronegative atom than molybdenum, tungsten should favor ligation of nitride relative to alkylidyne moieties, given the same set of ancillary ligands.[24] More importantly, the greater spatial extent of the d orbitals in W as compared to Mo should lead to a diminished barrier to metalacycle formation for W complexes.[24] This effect is noted both experimentally[25,26] and computationally[27] for AM. Further catalyst tuning was approached through variation of the ligand set. Employing weakly donating ligands such as OC(CF$_3$)$_2$Me and OCMe$_2$CF$_3$ serves two purposes. First, for a given metal, the use of weaker donor ligands favors the formation of an alkylidyne relative to the nitride. That is, for an identical set of ancillary ligands, there is a greater positive charge at the metal in the nitride complex than in the alkylidyne complex.[24] This charge is better supported when the ancillary ligands are strong donors. Thus, by stabilizing the alkylidyne relative to the nitride, the reformation of the alkylidyne from the nitride would be possible, as illustrated in Figure 1. Second, Schrock's investigations of alkyne metathesis by W complexes revealed that [2 + 2] cycloaddition to a terminal alkylidyne moiety becomes progressively more favorable as the degree of fluorination of the *t*-butoxide ligands increases because of increasing Lewis acidity of the W center.[25,26]

This effect is also borne out by DFT calculations of model systems, which indicate a stabilizing effect on the transition state for metalacyclobutadiene formation as the ancillary ligands

(10) Gdula, R. L.; Johnson, M. J. A. *J. Am. Chem. Soc.* **2006**, *128*, 9614.
(11) Zhang, W.; Kraft, S.; Moore, J. S. *J. Am. Chem. Soc.* **2004**, *126*, 329.
(12) Furstner, A.; Mathes, C.; Lehmann, C. W. *J. Am. Chem. Soc.* **1999**, *121*, 9453.
(13) Tsai, Y. C.; Diaconescu, P. L.; Cummins, C. C. *Organometallics* **2000**, *19*, 5260.
(14) Bunz, U. H. F. *Science* **2005**, *308*, 216.
(15) Fürstner, A.; Mathes, C. *Org. Lett.* **2001**, *3*, 221.
(16) Pschirer, N. G.; Bunz, U. H. F. *Tetrahedron Lett.* **1999**, *40*, 2481.
(17) Kaneta, N.; Hikichi, K.; Asaka, S.; Uemura, M.; Mori, M. *Chem. Lett.* **1995**, 1055.
(18) Mortreux, A.; Delgrange, J. C.; Blanchard, M.; Lubochinsky, B. *J. Mol. Catal.* **1977**, *2*, 73.
(19) Brizius, G.; Pschirer, N. G.; Steffen, W.; Stitzer, K.; zur Loye, H. C.; Bunz, U. H. F. *J. Am. Chem. Soc.* **2000**, *122*, 12435.
(20) North, M. Nitriles: General Methods and Aliphatic Nitriles. In *Comprehensive Organic Functional Group Transformations II*, 1st ed.; Katritzky, A. R., Taylor, R. J. K., Eds.; Elsevier: Amsterdam, 2005; Vol. 3, p 621.
(21) Tyrrell, E. Alkynes. In *Comprehensive Organic Functinal Group Transformations II*, 1st ed.; Katritzky, A. R., Taylor, R. J. K., Eds.; Elsevier: Amsterdam, 2005; Vol. 1, p 1083.
(22) Schrock, R. R.; Listemann, M. L.; Sturgeoff, L. G. *J. Am. Chem. Soc.* **1982**, *104*, 4291.
(23) Chisholm, M. H.; Folting, K.; Lynn, M. L.; Tiedtke, D. B.; Lemoigno, F.; Eisenstein, O. *Chem. Eur. J.* **1999**, *5*, 2318.
(24) Nugent, W. A.; Mayer, J. M. *Metal−Ligand Multiple Bonds*; John Wiley and Sons: New York, 1988; p 26.
(25) Freudenberger, J. H.; Schrock, R. R. *Organometallics* **1986**, *5*, 398.
(26) Schrock, R. R. *Acc. Chem. Res.* **1986**, *19*, 342.
(27) Zhu, J.; Jia, G.; Lin, Z. *Organometallics* **2006**, *25*, 1812.

Scheme 3. Syntheses of Tungsten-Nitride Complexes

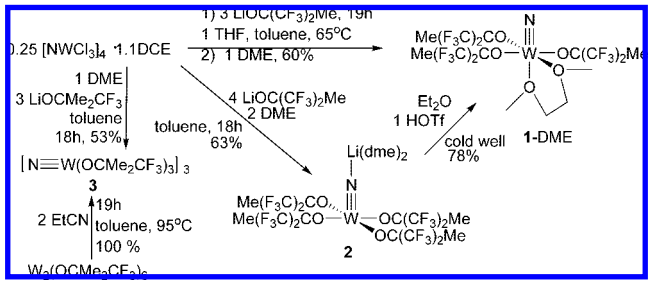

become poorer donors.[27] Degenerate N-atom exchange between nitriles, catalyzed by related complexes of Mo and W (Scheme 2), is thought to proceed via an analogous mechanism;[10,28] here too, the rate is enhanced by a more Lewis acidic metal center. Accordingly, we anticipated enhanced rates of reaction with the more highly fluorinated complex $N{\equiv}W(OC(CF_3)_2Me)_3$ (**1**) with respect to $[N{\equiv}W(OCMe_2CF)_3]_3$ (**3**).

Results and Discussion

Syntheses of Tungsten-Nitride Complexes. Our syntheses of the tungsten-nitride catalysts are depicted in Scheme 3. Treatment of $[N{\equiv}WCl_3]_4 \cdot 1.1DCE$[29] (DCE = 1,2-dichloroethane) with 16 equiv of $LiOC(CF_3)_2Me$ and 8 equiv of 1,2-dimethoxyethane (DME) in toluene afforded $[Li(DME)_2][N{\equiv}W(OC(CF_3)_2Me)_4]$ (**2**) in 63% yield. Subsequent treatment of **2** at low temperatures with CF_3SO_3H (HOTf) in diethyl ether afforded the DME adduct of $N{\equiv}W(OC(CF_3)_2Me)_3$, **1**-DME, in 78% yield. Alternatively, **1**-DME can be synthesized directly via the salt metathesis of $(N{\equiv}WCl_3)_4 \cdot 1.1DCE$ with 12 equiv of $LiOC(CF_3)_2Me$ in the presence of 4 equiv of THF at 65 °C to form a noncrystalline THF adduct of the desired species. Filtration of the reaction mixture followed by the addition of 4 equiv of DME to the filtrate then afforded crystalline **1**-DME in 60% yield from diethyl ether-pentane. This is the preferred method for multigram synthesis of **1**-DME, owing to the fact that the reaction of **2** with HOTf under standard conditions becomes less reliable when the quantity of **2** used exceeds 0.5 g. Similarly, $[N{\equiv}W(OCMe_2CF_3)_3]_3$ (**3**)[23] can be accessed via salt elimination with $LiOCMe_2CF_3$ in a 53% isolated yield. Additionally, we found that metathesis of $W_2(OCMe_2CF_3)_6$ with 2 equiv of propionitrile at 95 °C (but not at room temperature)[30] resulted in complete conversion to **3**.

Structures of Tungsten-Nitride Complexes. Single-crystal X-ray diffraction confirmed that **1**-DME is monomeric, unlike **3**, which exists as a trimer.[23] A thermal ellipsoid plot (Figure 2) reveals approximately octahedral coordination about W, with a characteristically short W≡N triple bond (Table 1). The DME ligand is bidentate, spanning sites trans to alkoxide and nitride ligands. Unsurprisingly, the W−O bond trans to the nitride ligand is substantially (0.305 Å) longer than that trans to alkoxide (Table 1), owing to the large trans influence of the triply bonded nitride ligand.[31] Complex **2** was likewise found to be monomeric, as determined by single-crystal X-ray diffraction. In this case, there were four crystallographically

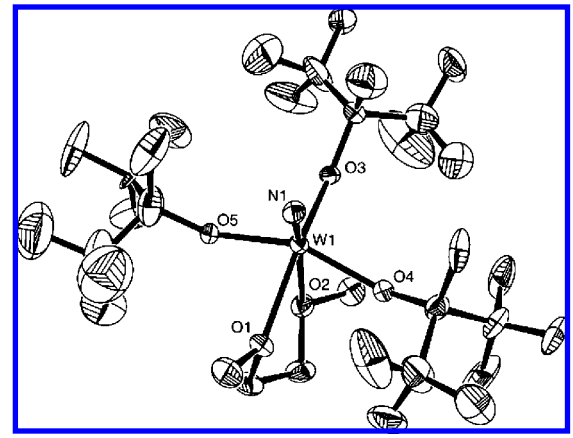

Figure 2. 50% thermal ellipsoid plot of catalyst precursor **1**-DME.

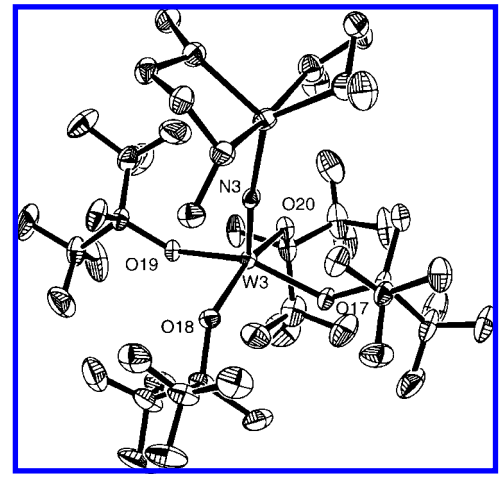

Figure 3. 50% thermal ellipsoid plot of catalyst precursor **2**.

Table 1. Selected Bond Lengths and Angles for **1**-DME and **2**

1-DME		2	
	Bond distances (Å)		
W−N	1.680(5)	W−N	1.672(1)
W−O(3)	1.906(3)	W−O(17)	1.9703(10)
W−O(5)	1.954(3)	W−O(18)	1.9569(10)
W−O(4)	1.949(3)	W−O(19)	1.9665(10)
W−O(1)	2.192(4)	W−O(20)	1.9640(10)
W−O(2) trans to N	2.483(4)	N−Li	2.063(3)
	Bond angles (deg)		
N−W−O(3)	105.20(14)	N−W−O(17)	102.23(5)
N−W−O(5)	102.00(14)	N−W−O(18)	100.17(5)
N−W−O(4)	100.70(14)	N−W−O(19)	102.18(5)
N−W−O(1)	97.85(14)	N−W−O(20)	100.31(5)
O(3)−W−O(5)	93.21(13)	O(18)−W−O(17)	87.81(4)
O(3)−W−O(4)	94.92(12)	O(18)−W−O(19)	88.10(4)
O(1)−W−O(4)	81.37(12)	O(20)−W−O(19)	87.96(4)
O(1)−W−O(5)	81.39(12)	O(20)−W−O(17)	87.53(4)
		W−N−Li	173.60(10)

independent molecules in each asymmetric unit. The $Li(DME)_2$ unit is directly coordinated to the nitride ligand as depicted in the thermal ellipsoid plot (Figure 3). Both **1**-DME and **2**, which are pale yellow in solution and colorless in the crystalline state, serve as sources of **1** in reactions with alkynes.

Syntheses of Tungsten-Alkylidyne Complexes. Both **1**-DME and **3** were dissolved in toluene-d_8 containing 3-hexyne to test for formation of the desired propylidyne complexes at room temperature. When **1**-DME was treated with 2 equiv of

(28) Chisholm, M. H.; Delbridge, E. E.; Kidwell, A. R.; Quinlan, K. B. *Chem. Commun.* **2003**, 126.
(29) Close, M. R.; McCarley, R. E. *Inorg. Chem.* **1994**, *33*, 4198.
(30) Freudenberger, J. H.; Pedersen, S. F.; Schrock, R. R. *Bull. Soc. Chim. Fr.* **1985**, 349.
(31) Nugent, W. A. *Metal−Ligand Multiple Bonds*; John Wiley and Sons: New York, 1988; p 156.

Scheme 4. Formation of Benzylidyne and Alkylidyne Complexes from **1**-DME

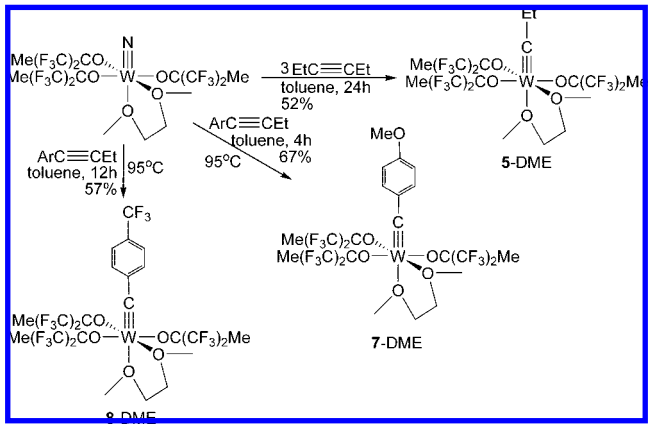

3-hexyne, an equilibrium mixture composed of 5 mol % tungstenacyclobutadiene complex $W(C_3Et_3)(OC(CF_3)_2Me)_3$ (**4**)[7] and 95 mol % propylidyne complex $EtC{\equiv}W(OC(CF_3)_2Me)_3(DME)$ (**5**-DME) was obtained after 20 h.[1] In the ^1H NMR spectra, the organic byproduct of the formation of **4** and **5**-DME, propionitrile, also was observed. In contrast, treatment of **3** with 10 equiv of 3-hexyne at room temperature did not result in the formation of detectable quantities of $EtC{\equiv}W(OCMe_2CF_3)_3$ (**6**). Furthermore, heating of the reaction mixture to 95 °C for several days resulted in only 9% conversion to **6**.

Taking advantage of the facile metathesis of **1**-DME with alkynes, we prepared several new alkylidyne complexes for further study. As depicted in Scheme 4, metathesis with 3-hexyne, 1-(4-methoxyphenyl)-1-butyne, and 1-(4-trifluoromethylphenyl)-1-butyne led to the successful isolation of **5**-DME (52%), $4\text{-MeO}(C_6H_4)C{\equiv}W(OC(CF_3)_2Me)_3(DME)$ (**7**-DME, 67%), and $4\text{-F}_3C(C_6H_4)C{\equiv}W(OC(CF_3)_2Me)_3(DME)$ (**8**-DME, 57%), respectively. Unlike with **1**-DME, the alkylidyne and benzylidyne analogues of **3** could not be synthesized directly from **3**, as very little conversion to the desired complexes was achieved even at 95 °C. Instead, $EtC{\equiv}W(OCMe_2CF_3)_3$ (**6**) was obtained via reaction of 3-hexyne with the ditungsten complex, $W_2(OCMe_2CF_3)_6$, as previously alluded to by Schrock.[30] Next, **6** was converted into the desired benzylidyne complexes $ArC{\equiv}W(OCMe_2CF_3)_3$ [Ar = C_6H_4OMe (**9**) or $C_6H_4CF_3$ (**10**)] via metathesis with the corresponding symmetrical alkynes in 83% and 73% yield, respectively (Scheme 5).

General Considerations for NACM. Because reversible formation of a nitride complex is required for the desired catalytic cycle, metathesis of propionitrile with the propylidyne species was analyzed. Metathesis of **5**-DME with propionitrile at 95 °C led to a 28% conversion to **1**-DME in 3 h. Unlike **5**-DME, complex **6** was completely converted to **3** upon addition of propionitrile and heating at 95 °C, although some decomposition to $O{=}W(OCMe_2CF_3)_4$ (**11**) was noted. This decomposition likely occurred via C−O bond scission, as unidentified volatile fluorine-containing materials were observed upon vacuum transfer of the volatile materials from the reaction mixture. C−O bond scission in alkoxide ligands is known to afford terminal oxo complexes.[32] Redistribution of the alkoxide ligands is required for the formation of **11**. Successful isolation of **11** in

(32) Mayer, J. M. *Polyhedron* **1995**, *14*, 3273.

Scheme 5. Formation of Benzylidyne and Alkylidyne Complexes

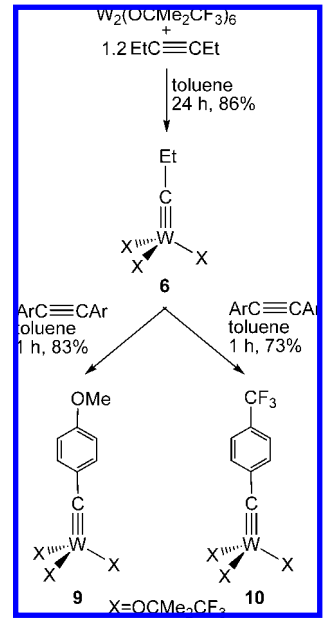

24% yield occurred when **3** was heated at 95 °C in the presence of 3-hexyne. No other tungsten-containing products were identified.

Once reversible formation of **1**-DME was established, we sought to exploit this property for the exchange of R and R′ units in an alkyne (RC≡CR) and a nitrile (R′C≡N). The nitride complexes were chosen over the corresponding tungsten-propylidyne complexes as the starting form of the catalyst. This was due to the facility with which the metal nitrides could be synthesized in comparison to their propylidyne counterparts. Initial test reactions were conducted with *p*-methoxybenzonitrile and 0.5 equiv of 3-hexyne in the presence of **1**-DME (5 mol% based on *p*-methoxybenzonitrile) at 95 °C. After 21 h, ^1H NMR spectroscopy indicated conversion to bis(4-methoxyphenyl)acetylene (77%), 1-(4-methoxyphenyl)-1-butyne (15%), with some remaining *p*-methoxybenzonitrile (8%) along with the N-containing byproduct, propionitrile (eq 1).

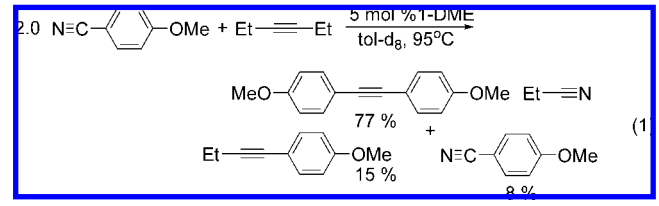

Since **2** could potentially serve as a source of **1** in solution, **2** also was tested for NACM activity. Complex **2** was found to be active, albeit with lower yields and longer reaction times than **1**-DME.[1] Similarly, given that trace amounts of propylidyne complex were observed upon prolonged heating of **3** in the presence of 3-hexyne, **3** was tested for NACM activity. Successful conversion of the aryl nitrile to aryl alkyne was observed with **3**, although overall yields were lower and the metathesis reaction occurred at a slower rate than with **1**-DME.[1] The slower rate of metathesis is consistent with trends in AM rates, where the rate of metathesis increases as the pK_a of conjugate acids of the alkoxide ligands decreases.[7]

Surprisingly, eq 1 shows that the symmetrical diaryl alkyne is the major alkyne produced. This is not the primary product

Scheme 6. Three Possible Cycles for Formation of Symmetrical Alkyne

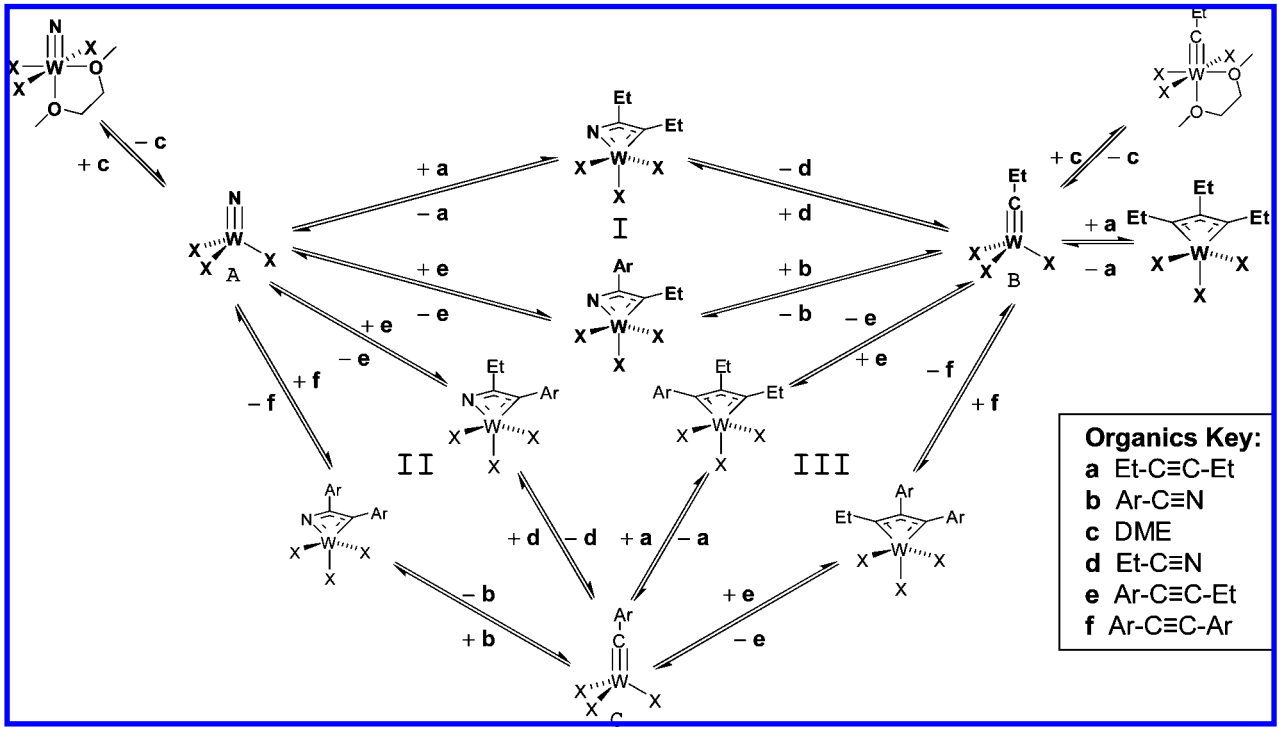

of NACM but must arise from a secondary transformation. In principle, three different triple-bond metathesis cycles can contribute to the formation of the symmetrical alkyne product. These are illustrated in Scheme 6. For simplicity, the organic reactants and products are denoted as **a**−**f**. Key metal complexes are denoted as **A**−**C**. This focuses attention on the numerous metal complexes involved in the three coupled cycles. At the beginning of the catalytic cycle (cycle I), metathesis of nitrido complex **A** with 3-hexyne (**a**) led to the formation of propylidyne complex **B** with concomitant release of propionitrile (**d**). The unsymmetrical alkyne (**e**) then was formed initially by NACM via reaction between the propylidyne complex **B** and aryl nitrile (**b**), with concomitant regeneration of the nitride complex (Scheme 6, cycle I). The symmetrical alkyne (**f**) is a secondary product that can be subsequently formed via either NACM (cycle II) or ACM (cycle III) of the unsymmetrical alkyne (**e**). Only NACM can account for the transformation of the aryl nitrile (**b**) into an aryl alkyne (**e**); ACM can only equilibrate the various alkynes after they are formed. Thus, NACM is critical to the complete catalytic cycle.

At this point, it was unclear as to whether the symmetrical alkyne (**f**) is formed predominantly through ACM or NACM or a combination of the two processes. To better understand the role of ACM and NACM in the generation of symmetrical alkyne, the aforementioned alkylidyne and benzylidyne complexes ligated with either $OC(CF_3)_2Me$ (**5**-DME, **7**-DME, and **8**-DME) or $OCMe_2CF_3$ (**6**, **9**, and **10**) were used to investigate the feasibility and reversibility of each proposed cycle.

Reversibility of NACM and ACM Steps. NACM Cycle I. NACM Cycle I is depicted separately from the other cycles in Scheme 7. Table 2a−d summarizes the results of stoichiometric investigations of the proposed pathways for the formation of unsymmetrical alkynes via NACM with both **1**-DME and **3** at 95 °C (Scheme 7). As expected, each step contributing to the formation of the unsymmetrical alkyne operates reversibly for both catalysts. However, the catalyst resting state varies greatly

Scheme 7. NACM Cycle I (Formation of ArC≡CEt from ArC≡N)

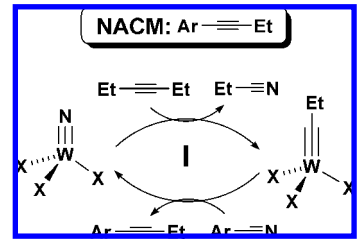

as a function of the ancillary ligands. Use of the less electron-donating $OC(CF_3)_2Me$ ligand leads to preferential formation of alkylidyne or benzylidyne complexes. In contrast, the nitride complex is favored when $OC(CF_3)Me_2$ ligands are employed. Furthermore, formation of benzylidyne was favored over that of propylidyne with both catalysts. Table 2c,d reveals no significant electronic influence on the catalyst resting state as a function of the para-substitution on the aryl group of the substrates. Table 2a examines the formation of the tungsten-propylidyne (**5**-DME and **6**) complexes and propionitrile upon treatment of the corresponding tungsten-nitride complexes with 3-hexyne. Table 2b examines the reverse reaction. The fact that the final compositions differ for these forward and reverse reactions is a consequence of the operation of two other processes, in addition to the highlighted triple-bond metathesis. First, alkyne polymerization (AP) preferentially consumes small alkyl-substituted alkynes (i.e., 3-hexyne) from the mixture over time, as noted previously.[1] Second, close inspection of the reaction mixtures reveals some decomposition of the tungsten complexes, resulting in the formation of oxo complexes of the form $W(O)(OR)_4$ (**11**). As noted, C−O bond scission in the alkoxide ligands appears to be the origin of the oxo ligands. Ligand redistribution must account for the extra alkoxide ligands in **11**. Not all the tungsten can be accounted for. In comparing the reversible formation of nitride from alkylidyne species for the $W(OC(CF_3)_2Me)_3$ fragment (Table 2a vs b), a large

Table 2

(a) N≡[W] + EtC≡CEt → EtC≡[W] + EtC≡N

entry	catalyst	W≡N	W=O	W≡CR, W(C_3R_3)
1	**3**	63	26	9
2	**1**-DME[a]	0	0	100

(b) N≡[W] + EtC≡CEt ← EtC≡[W] + EtC≡N

entry	catalyst	W≡N	W=O	W≡CR, W(C_3R_3)
1	**6**	89	11	0
2	**5**-DME	28	0	72

(c) N≡[W] + *p*-XC_6H_4C≡CEt → EtC≡[W] + *p*-XC_6H_4C≡N

entry	catalyst	X	W≡N	W=O	W≡CR, W(C_3R_3)	W≡CAr
1	**3**	OMe	75	14	0	9
2	**1**-DME	OMe	6	0	14	80
3	**3**	CF_3	42	33	0	25
4	**1**-DME	CF_3	13	0	0	87

(d) N≡[W] + *p*-XC_6H_4C≡CEt ← EtC≡[W] + *p*-XC_6H_4C≡N

entry	catalyst	X	W≡N	W=O	W≡CR, W(C_3R_3)	W≡CAr
1	**6**	OMe	60	9	0	25
2	**5**-DME	OMe	12	0	10	78
3	**6**	CF_3	64	5	4	19
4	**5**-DME	CF_3	13	0	0	87

[a] Room temperature.

Scheme 8. NACM Cycle II (Secondary Formation of ArC≡CAr)

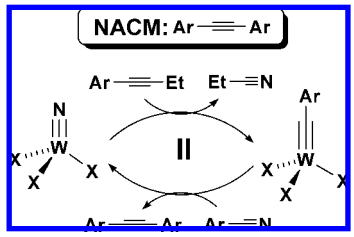

difference in catalyst resting state is observed. The conversion of the nitride to the alkylidyne species readily occurs at room temperature. In contrast, the conversion of the alkylidyne to the nitride unit is slow and occurs only at elevated temperatures. Trace amounts of nitride complex are probably formed under these conditions, with 3-hexyne being removed from the system via slow AP, which in turn shifts the solution composition. Thus, the same equilibrium is not established in these two cases, owing to varying quantities of CEt units present in the various soluble species. The impact of AP on the system is discussed in greater detail later.

NACM Cycle II (Scheme 8). Scheme 8 focuses on NACM cycle II. Similar catalyst resting state patterns were observed when analyzing the steps of NACM to form the symmetrical alkyne at 95 °C, as shown in Table 3a−d. With **3**, larger amounts of the terminal oxo complex **11** were generally observed at extended reaction times under heating. Interestingly, unlike NACM cycle I (to form the unsymmetrical alkyne), one segment of cycle II appeared to be irreversible with catalyst **3**. As indicated in Table 3c (entry 3), treatment of **3** with bis(4-trifluoromethyl)acetylene resulted in no conversion to **10.** The corresponding entry in Table 3d indicates that the reverse reaction occurs essentially quantitatively except for some catalyst decomposition. Only slight conversion is observed with the *p*-methoxy derivative, but entry 1 in Table 3c,d clearly indicates

Table 3

(a) N≡[W] + *p*-XC_6H_4C≡CEt → *p*-XC_6H_4C≡[W] + EtC≡N

entry	catalyst	X	W≡N	W=O	W≡CAr	W≡CR, W(C_3R_3)
1	**3**	OMe	75	14	9	0
2	**1**-DME	OMe	6	0	80	14
3	**3**	CF_3	42	33	25	0
4	**1**-DME	CF_3	13	0	87	0

(b) N≡[W] + *p*-XC_6H_4C≡CEt → *p*-XC_6H_4C≡[W] + EtC≡N

entry	catalyst	X	W≡N	W=O	W≡CAr	W≡CR, W(C_3R_3)
1	**9**	OMe	70	7	14	0
2	**7**-DME	OMe	42	0	39	19
3	**10**	CF_3	61	11	21	0
4	**8**-DME	CF_3	17	0	83	0

(c) N≡[W] + *p*-XC_6H_4C≡C-*p*-C_6H_4X → *p*-XC_6H_4C≡[W] + *p*-XC_6H_4C≡N

entry	catalyst	X	W≡N	W=O	W≡CAr
1	**3**	OMe	76	17	7
2	**1**-DME[a]	OMe	46	0	54
3	**3**	CF_3	100	0	0
4	**1**-DME	CF_3	67	0	33

(d) N≡[W] + *p*-XC_6H_4C≡C-*p*-C_6H_4X ← *p*-XC_6H_4C≡[W] + *p*-XC_6H_4C≡N

entry	catalyst	X	W≡N	W=O	W≡CAr
1	**9**	OMe	90	10	0
2	**7**-DME	OMe	49	0	51
3	**10**	CF_3	86	14	0
4	**8**-DME	CF_3	65	0	35

[a] Room temperature.

Scheme 9. ACM (Cycle III, Formation/Consumption of ArC≡CAr)

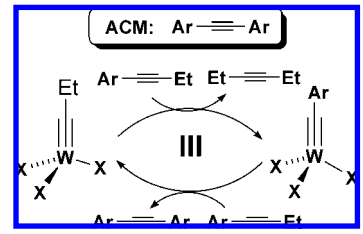

reversibility in this latter case. In contrast, the use of **1**-DME affords substantial quantities of both nitride and alkylidyne complexes at equilibrium, without the formation of the terminal oxo decomposition product. Once again, differential AP and C−O bond scission prevents establishment of the same equilibrium for forward and reverse reactions in the three cases where both forward and reverse reactions operate.

ACM (Cycle III, Scheme 9). The ACM cycle (cycle III) is highlighted in Scheme 9. Table 4a−d summarizes the results obtained for cycle III, tungsten-catalyzed ACM. Tungsten-catalyzed ACM is well-studied both experimentally and computationally,[5,7,27] so it was unsurprising to find that these steps are reversible at room temperature. An analysis of the steps of ACM in the production of the symmetrical alkyne revealed that the two catalyst systems behaved similarly at room temperature. In the case of the catalyst based on $OC(CF_3)Me_2$ ligands, the ratio of benzylidyne to propylidyne complexes was often not determined because of the presence of multiple overlapping resonances in the ^{1}H NMR spectra. These arose from other unidentified species (likely metalacycles) that appeared upon cooling the samples. As a result, only the presence of these species in solution is indicated in Table 4a−d.

Table 4

(a) EtC≡[W] + *p*-XC_6H_4C≡CEt → *p*-XC_6H_4C≡[W] + EtC≡CEt

entry	catalyst	X	W≡CR, W(C_3R_3)	W≡CAr
1	**6**	OMe	present	present
2	**5**-DME	OMe	31	69
3	**6**	CF_3	35	65
4	**5**-DME	CF_3	21	79

(b) EtC≡[W] + *p*-XC_6H_4C≡CEt ← *p*-XC_6H_4C≡[W] + EtC≡CEt

entry	catalyst	X	W≡CR, W(C_3R_3)	W≡CAr
1	**9**	OMe	present	present
2	**7**-DME	OMe	52	48
3	**10**	CF_3	33	67
4	**8**-DME	CF_3	49	51

(c) EtC≡[W] + *p*-XC_6H_4C≡C-*p*-C_6H_4X → *p*-XC_6H_4C≡[W] + *p*-XC_6H_4C≡CEt

entry	catalyst	X	W≡CR, W(C_3R_3)	W≡CAr
1	**6**	OMe	trace	100
2	**5**-DME	OMe	6	93
3	**6**	CF_3	0	100
4	**5**-DME	CF_3	16	84

(d) EtC≡[W] + *p*-XC_6H_4C≡C-*p*-C_6H_4X ← *p*-XC_6H_4C≡[W] + *p*-XC_6H_4C≡CEt

entry	catalyst	X	W≡CR, W(C_3R_3)	W≡CAr
1	**9**	OMe	present	present
2	**7**-DME	OMe	20	80
3	**10**	CF_3	trace	100
4	**8**-DME	CF_3	0	100

Note that as usual, the difference in ratios in catalyst resting states for the forward and reverse reactions is due to the lack of well-defined equilibrium conditions as a result of the competing irreversible AP. Overall, the favored resting state of the catalysts was the benzylidyne complex. In contrast with NACM (cycles I and II), all ACM reactions occurred rapidly at room temperature. Furthermore, the identity of the para-substituent on the aryl substrate did not appear to exert a significant influence on the catalyst resting state with ACM.

Overall, these stoichiometric studies suggest three major conclusions. First, the large difference in reaction rate between NACM and ACM at room temperature implicates ACM as the primary process by which the symmetrical alkyne is formed over NACM (i.e., the symmetrical diaryl alkyne is formed principally via cycle III and not cycle II, at least in the case of ligation by $OC(CF_3)_2Me$). Second, given the rapidity of ACM relative to NACM irrespective of the alkoxide ligand used, the difference in the ratio of symmetrical to unsymmetrical alkynes observed with the two catalysts (**1**-DME vs **3**) under NACM conditions is likely due to the difference in the resting states of the catalysts. In particular, the use of $OC(CF_3)Me_2$ ligands suppresses ACM by virtue of the fact that the NACM catalyst resting state is the terminal nitride complex. This means that the alkylidyne complexes required for ACM are present in only very small quantities. When the alkoxide ligands used are $OC(CF_3)_2Me$, a much larger fraction of the catalyst exists in the alkylidyne form, thus favoring rapid ACM. Last, although electronic influences of the aryl substrate do not appear to have a strong impact on the catalyst resting state in ACM, more subtle effects did render one step in NACM irreversible with catalyst **3**, underscoring the complexity of the system.

To confirm the relative facility of NACM and ACM, another substrate set was examined. Here, the reaction of 3,5-dimethylbenzonitrile, bis(4-methyoxyphenyl)acetylene, and 3-hexyne in the presence of **1**-DME or **3** at 95 °C in toluene was monitored via ^{1}H NMR spectroscopy (Scheme 10). An equilibrium mixture of ACM products was observed within 10 min when catalyst **1**-DME was used; there was no evidence of NACM products at this time.[1] In the case of catalyst **3**, only ACM products were noted after 10 min, but the reaction had not yet reached equilibrium. After 3 h, NACM products began to predominate in the reaction mixtures for both catalysts. This revealed that ACM occurred at a much faster rate than NACM for both catalysts under these conditions. Therefore, the overall process for producing a symmetrical alkyne can be described as NACM to produce an unsymmetrical alkyne followed by rapid ACM to generate the symmetrical alkyne as depicted in Scheme 11.

Scheme 10. Formation of ACM versus NACM Products

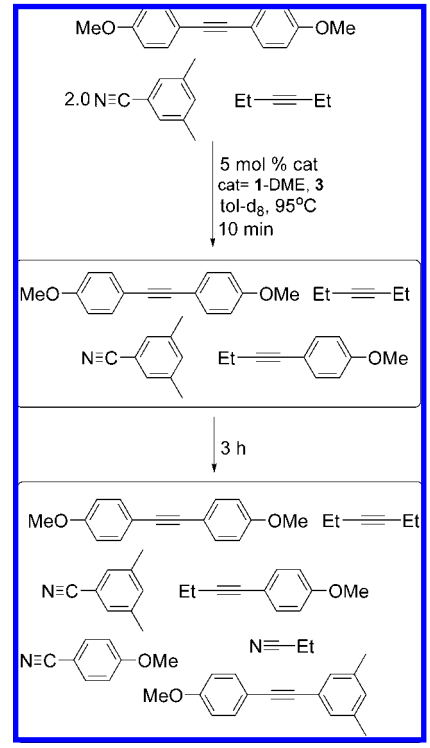

DFT Calculations of NACM Mechanism. Calculations on a model system support a relatively low-energy [2 + 2] cycloaddition−cycloreversion mechanism for NACM (Scheme 12). The calculations were carried out at the DFT level, employing the commonly used B3LYP functional[33–35] and the LACVP* basis set.[36] The Jaguar 6.5 package[37] was used to implement the calculations. Coordinates for all atoms in the optimized structures and associated bond lengths and angles are listed in the Supporting Information. The experimental $OC(CF_3)_xMe_{3-x}$ (x = 1, 2) ligands were modeled by OMe. No constraints were employed in calculating the transition states; these stationary points involve only a single imaginary frequency. All transition states were verified to form the corresponding reactant and product by geometry optimization along

(33) Becke, A. D. *J. Chem. Phys.* **1993**, *98*, 5648.
(34) Vosko, S. H.; Wilk, L.; Nusair, M. *Can. J. Phys.* **1980**, *58*, 1200.
(35) Lee, C. T.; Yang, W. T.; Parr, R. G. *Phys. Rev. B: Condens. Matter Mater. Phys.* **1988**, *37*, 785.
(36) Hay, P. J.; Wadt, W. R. *J. Chem. Phys.* **1985**, *82*, 299.
(37) Schrodinger, L. L. C. *Jaguar 6.5*; New York, 2005.

Scheme 11. Preferred Pathways for Formation of Symmetrical Alkynes

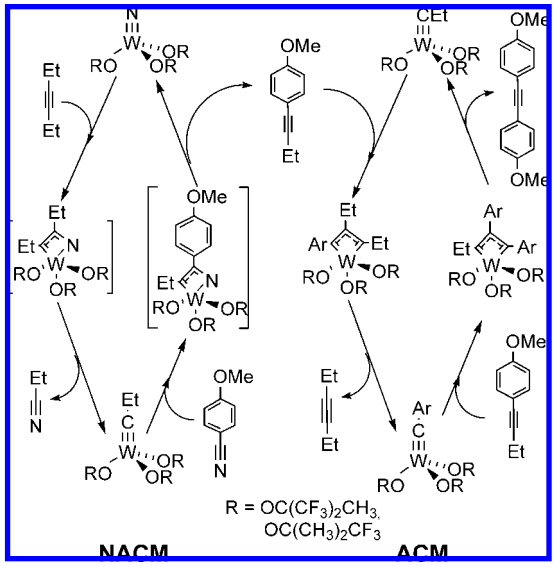

the associated reaction coordinate. Energy values are reported as ΔG values that have been corrected for zero point energies.

Examination of Scheme 12, which corresponds to the tungsten nitride → tungsten alkylidyne transformation in Scheme 7, reveals several important points. Two distinct azatungstenacyclobutadiene intermediates (**Int 1** and **Int 2**) are discernible. These are relatively high-energy species, not more than 5.1 kcal mol^{-1} more stable than the corresponding transition states for the approach of MeC≡CMe to W(≡N)$(OMe)_3$ (**TS 1**) or the approach of MeC≡N to W(≡CMe)$(OMe)_3$ (**TS 3**). Both **Int 1** and **Int 2** feature significant bond localization in the W−N−C−C ring. The calculated metrical parameters correspond approximately to W=N−C=C−W bonding in **Int 1** in contrast to the W−N=C−C=W bond alternation in **Int 2**. These intermediates are best described as having distorted square pyramidal structures (τ = 0.34 and 0.14, respectively[38]) with the three methoxide ligands occupying basal positions. In **Int 1** and **Int 2**, the atom with the tungsten-element double bond occupies the apical position. The trans influence is a likely explanation for this preference.

The reactants N≡W$(OMe)_3$ + MeC≡CMe are isoenergetic with products MeC≡W$(OMe)_3$ + MeC≡N in this model system, which, together with reasonable activation barriers, explains the reversibility of the NACM reaction. Note that in the experimental systems, the weaker electron-donating ability of the fluorinated alkoxide ligands as compared to OMe (the model ligands) should decrease the barriers to metalacycle formation and stabilize the alkylidyne complex relative to its nitride analogue. Indeed, in the experimental systems, the use $OCMe_2CF_3$ ligands leads to the nitride complex as the only detectable W-containing species under catalytic conditions. In contrast, alkylidyne complexes are generally favored when the ancillary ligands are $OC(CF_3)_2Me$.

Analysis of the transition state motions allows for better understanding of the mechanism (Figure 4). **TS 1** defines the formation of the azatungstenacyclobutadiene via [2 + 2] cycloaddition of alkyne to the tungsten-nitride complex. Only the nitrogen and two carbon atoms that form the azametalacycle

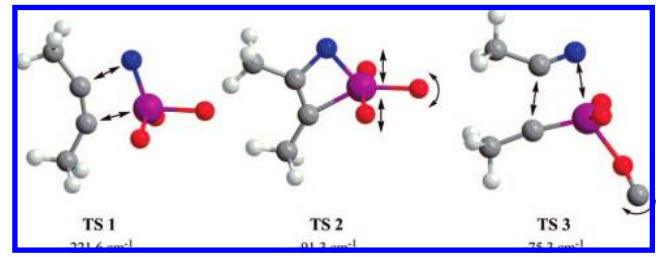

Figure 4. Calculated vibrational transition state motions. Me groups of OMe ligands were removed for clarity if associated atoms showed no significant motion during the transition state.

account for significant molecular motion in this transition state. This transition state is the maximum energy on the reaction coordinate diagram and thus controls the rate of the NACM reaction.

TS 2 is the transition state that connects the two distinct azametalacyle intermediates **Int 1** and **Int 2**. The geometry of **TS 2** is intermediate between the trigonal bipyramidal (tbp) and square pyramidal (sp) extremes. In this case, use of τ is somewhat deceptive, owing to the constraints of the azametalacyclobutadiene ring. The ring enforces a small N−W−C_α angle (in **TS 2**, 79.9°), which necessarily leads to at least one large (>140°) angle in the N−C_α−O_e plane. Consequently, the maximum value of τ possible in this case is 0.67 rather than 1. Examination of Scheme 12 reveals that it is most instructive to regard **TS 2** as the tbp structure that connects the two sp azametalacycles **Int 1** and **Int 2**. In **TS 2**, the O_a−W−O_a angle assumes its maximum value (165.6°), dramatically larger than the corresponding angle in **Int 1** (144.5°) or **Int 2** (148.4°). In **TS 2**, these O atoms define the axial sites in the distorted tbp structure.

The atomic motions involved in the **Int 1** → **TS 2** → **Int 2** conversion are best described as consisting of the methoxide ligand O_eMe moving from a basal site in sp **Int 1**, where it is trans to C_α, to a basal site trans to the N atom in sp **Int 2** by passing between the other two OMe ligands— a "swing-through" mechanism. The bonds in the metalacycle change as shown in Figure 4 such that the "apical" atom in the sp structures has the greater multiple-bond character in its interaction with W. The vibrational motions described by the single imaginary frequency in **TS 2** consist of an "umbrella inversion" of the C_tO_3 unit about W as the O_a−W−O_a angle opens to permit O_eMe to pass through. Metrical parameters for **TS 2** are more similar to those of **Int 1** than **Int 2**; **TS 2** resembles **Int 1** more closely than **Int 2**. This also is reflected in the (admittedly deceptive) τ parameters for these three structures.

TS 3 defines the [2 + 2] cycloreversion to yield the tungsten-ethylidyne complex and acetonitrile. As seen for **TS 1**, the nitrogen and two carbon atoms of azatungstenacyclobutadiene show significant motion in the transition state vibration; some rotation about the W−O_e bond also contributes to this transition state. To the extent that W(≡N)$(OMe)_3$ is electronically similar to W(≡CMe)$(OMe)_3$, the principle of microscopic reversibility requires that the entering/departing organic substrates in **TS 1** and **TS 3** must approach/leave the W≡E (E = N, CMe) bond in analogous orientations. This criterion is met by these two transition states, wherein each E occupies the apical position in an approximately square-pyramidal structure. This in turn necessitates the swing-through interconversion of sp **Int 1** with sp **Int 2** via tbp **TS 2**.

Directly comparable DFT calculations for (degenerate) alkyne metathesis of the model complex W(≡CMe)$(OMe)_3$ with

(38) Addison, A. W.; Rao, T. N.; Reedijk, J.; Vanrijn, J.; Verschoor, G. C. *J. Chem. Soc., Dalton Trans.* **1984**, 1349.

Scheme 12. Calculated Structures and Relative Gibbs Energies (kcal mol^{-1}) for Nitride-Alkylidyne Interconversion in a Model System[a]

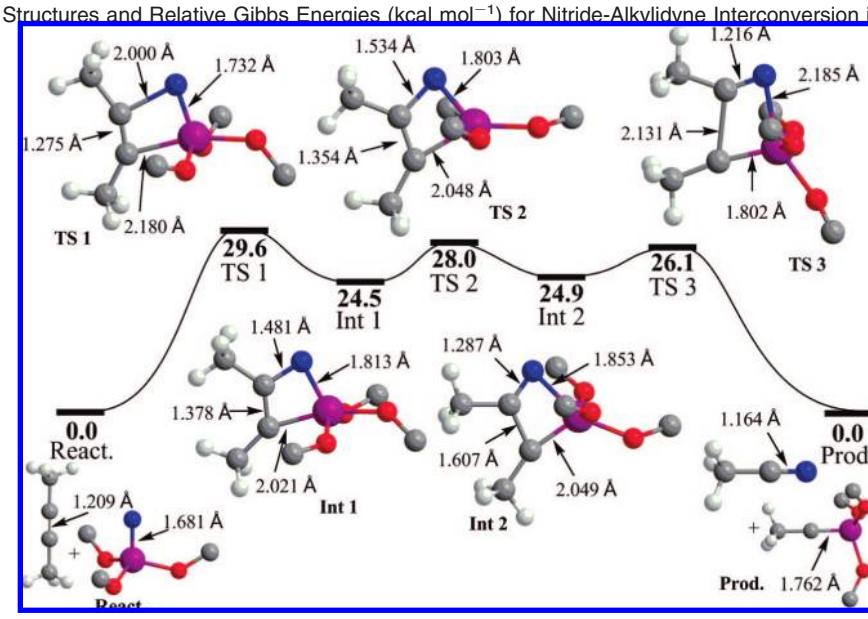

[a] H atoms of OMe ligands have been removed for clarity.

MeC≡CMe were reported recently.[27] In that case, two distinct metalacycles with bond alternation also were found,[39] although they are substantially more stable than the azametalacycles that we calculate for NACM. Likewise, the energy of the highest-lying transition state in that model ACM system is only 22.3 kcal mol^{-1} greater than the reactants,[27] as compared to 29.6 kcal mol^{-1} in the case of NACM. This agrees qualitatively with our experimental findings that ACM proceeds much more rapidly than NACM with current catalysts.

Direct Monitoring of Catalytic Reaction Progress. The catalyst resting state and reaction progress were monitored via NMR spectroscopy to examine the practical consequences of the difference in relative stability of the metal-nitride and metal-alkylidyne forms of catalysts **1**-DME and **3**. ^{1}H NMR spectroscopic monitoring of most NACM reactions proved unsuitable because of difficulties in deconvoluting multiple overlapping resonances. Therefore, these studies involved the metathesis of *p*-trifluoromethylbenzonitrile and 3-hexyne at 95 °C and were monitored by ^{19}F NMR spectroscopy. Spectra were collected every 5 min over a 2 h reaction time for catalysts **1**-DME and **3**.

Owing to technical limitations as well as the complexity of the coupled NACM-ACM-AP processes operating in these systems, these initial studies have resisted attempts to extract rate constants. Nevertheless, these ^{19}F NMR studies revealed several important qualitative differences in reactivity between the two catalysts, **1**-DME and **3**. The rate of formation of the symmetrical alkyne from an unsymmetrical alkyne was found to be much more rapid with **1**-DME than with **3**. The symmetrical and unsymmetrical alkyne distribution was nearly that established by ACM alone throughout the reaction catalyzed by **1**-DME. In contrast, the reaction with **3** resulted in a buildup of an unsymmetrical alkyne prior to its conversion to a symmetrical alkyne; the alkynes were not in the equilibrium ratio expected on the basis of rapid ACM. Furthermore, the catalyst resting state of **1**-DME under these catalytic conditions consists of a mixture of **1**-DME, **5**-DME, and **8**-DME, with gradual funneling toward the benzylidyne complex **8**-DME as the reaction proceeds. Examination of the spectra obtained for the reaction catalyzed by **3** does not permit unambiguous assignment of the resting state in this system. However, it is not **3**, **6**, or **10**. Instead, the catalyst resting state under these conditions appears to be an adduct of **3**, as no aryl or alkyl peaks corresponding to benzylidyne or alkylidyne complexes were observed in the ^{1}H NMR spectrum. Additionally, the aforementioned studies of NACM pathways further support a nitride complex as the catalyst resting state. The presence of a nitride complex as the sole catalyst resting explains the greater accumulation of the unsymmetrical alkyne. This is because ACM requires a metal-alkylidyne catalyst, which is present only in very low concentrations when the bulk of the catalyst exists in the nitride form. Thus, the use of **3** results in significant decoupling of the NACM and ACM processes. This suppresses the rate of formation of the secondary product, the diaryl alkyne.

Preferential Formation of Symmetrical Alkynes. From our initial study of NACM (eq 1), it can be noted that the alkyne product is largely composed of the symmetrical alkyne. While ACM accounts for the formation of the symmetrical species, it cannot by itself account for the selectivity of the system. There are two reasonable explanations for the preferential formation of the symmetrical alkyne. From a thermodynamic perspective, the formation of an unsymmetrical alkyne from 3-hexyne and benzonitrile is enthalpically favored in the gas phase: $\Delta H^\circ = -5.8$ kcal mol^{-1} (eq 2).[40] More importantly, the formation of the symmetrical alkyne from the same precursors is more than twice as favorable, with $\Delta H^\circ = -13.2$ kcal mol^{-1} (eq 4)[40]

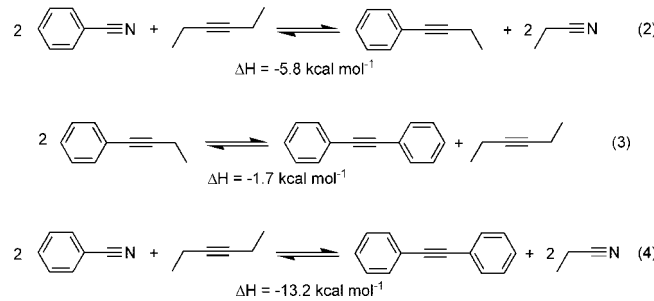

(39) Metalacycles are equivalent due to the degenerate nature of the ACM reaction modeled.

In addition to the thermodynamic preference of the system, a concurrent side reaction, AP, also favors the formation of the symmetrical alkyne. AP shifts the equilibrium of the system toward the formation of symmetrical alkynes by removing 3-hexyne from the reaction mixture as a polymer. Indirect evidence of AP can be found under conditions where complete consumption of 3-hexyne occurs with incomplete conversion of the nitrile into alkyne, suggesting that some of the 3-hexyne must have been removed from the system via an alternative mechanism. The direct evidence, polymer, is observed as copious insoluble material under the reaction conditions.

Effects of Catalyst Loading and Temperature. Although AP drives the formation of symmetrical alkynes, it can also be detrimental to the system in that it consumes 3-hexyne without producing the desired alkyne product. Accordingly, the system was optimized in toluene at 95 °C with 5 mol % catalyst loadings and 1 equiv of 3-hexyne to determine the conditions that would favor NACM over AP. Optimal NACM yields and rates were obtained when catalyst concentrations of 6 and 35 mM **1**-DME and **3**, respectively, were employed.[1] Additional studies with the more reactive catalyst, **1**-DME, were completed in which the temperature and catalyst loading in toluene were varied (eq 5, $n = 1$).[1] As the temperature was decreased, reaction yields and rates decreased dramatically. Meanwhile, increasing catalyst loadings led to increased rates of reaction, as anticipated

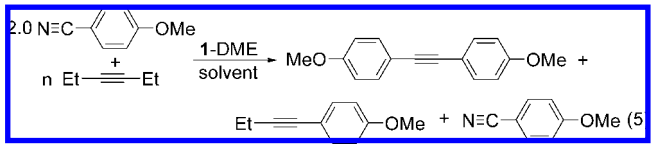

Effect of Excess 3-Hexyne. The impact of the quantity of 3-hexyne on yields and rates of the reaction defined by eq 5 in toluene also was investigated.[1] Use of a moderate excess of 3-hexyne (2−3 equiv) with nitriles that otherwise reacted sluggishly increased overall rates and yields of alkyne products. Furthermore, reactions could be performed at lower temperatures with excess 3-hexyne to afford increased yields of the desired alkynes. Naturally, as the amount of 3-hexyne introduced into the system was increased, the selectivity for formation of symmetrical alkynes greatly decreased as a direct result of the ACM equilibrium. When **1**-DME was used as the catalyst, good yields of the symmetrical alkyne could nevertheless be obtained in these cases by taking advantage of AP as described next.

Consequences of AP. As expected, reaction mixtures containing even a slight excess of 3-hexyne often afforded increased quantities of unsymmetrical alkynes relative to symmetrical alkynes. However, simply removing the volatiles from the system after complete conversion of the nitrile to a mixture of alkynes, followed by resubjection of the resulting residue to standard reaction conditions (toluene, 95 °C), resulted in nearly complete conversion of the unsymmetrical alkyne to the symmetrical alkyne via tandem ACM-AP with **1**-DME (Scheme 13). Interestingly, with catalyst **3**, no conversion of the unsymmetrical alkyne to the symmetrical alkyne was observed under these reaction conditions. The inability to shift the product ratio with **3** is likely due to the catalyst resting state in the residue. As noted previously, the resting state of catalyst **3** appears to

Scheme 13. Harnessing AP to Form Symmetrical Alkynes

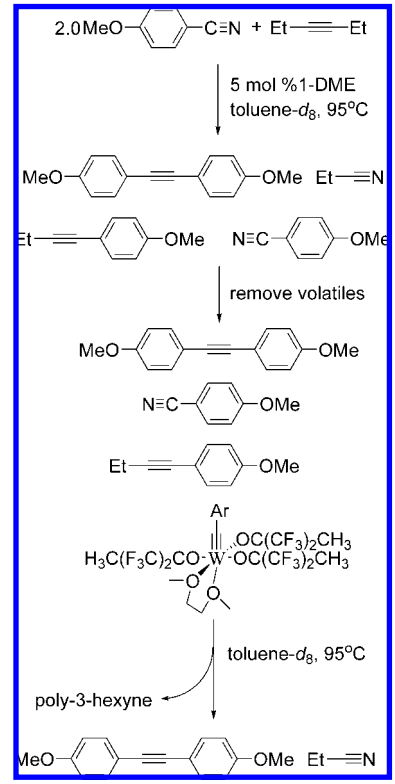

be some form of the nitride complex. If so, the low concentration of the metal-alkylidyne complex must preclude AP under the tested conditions. It has been suggested that AP occurs via ring expansion of metalacyclobutadiene complexes,[7,11] although there are other possibilities such as the formation of metal-alkylidene complexes.[41,42]

Comparison of Catalysts. The divergent behavior of the reaction mixtures with respect to tandem ACM-AP following apparent completion of NACM for the two cases of catalysis by **1**-DME and catalysis by **3** prompted us to examine this behavior more closely. After the NACM reaction catalyzed by **1**-DME had neared its end point as judged by ^{1}H NMR spectroscopy, to the resulting mixture of alkynes and propionitrile was added excess propionitrile. The NMR tube was then resealed and heated to 95 °C. Reformation of 18% aryl nitrile after 23 h clearly indicated the reversibility of NACM (Scheme 14) in this case. In contrast, when **3** was used as the catalyst, extensive broadening of the NMR signals owing to polymer formation necessitated filtration and removal of volatile materials from the filtrate. Upon reconstitution in toluene and addition of propionitrile to the resulting product mixture, the reformation of aryl nitrile did not occur. Under these conditions, the "back reaction" of the alkynes ArC≡CEt and ArC≡CAr with EtCN did not occur; NACM was irreversible with this catalyst. This result is consistent with our earlier observation that the resting state of **3** appears to be a nitride complex, as indicated by the buildup of unsymmetrical alkyne with **3** (diminished ACM) and the much more sluggish NACM activity of catalyst **3** in comparison to **1**-DME. It also is consistent with failure to observe any reaction of **3** with ArC≡CAr under stoichiometric conditions (Table 3c, entry 3).

(40) NIST Chemistry WebBook−National Institute Standard Reference Database Number 69; June 2005 release. http://webbook.nist.gov/chemistry/

(41) Mortreux, A.; Petit, F.; Petit, M.; Szymanskabuzar, T. *J. Mol. Catal. A: Chem.* **1995**, *96*, 95.

(42) Masuda, T.; Sasaki, N.; Higashimura, T. *Macromolecules* **1975**, *8*, 717.

Scheme 14. Reversibility Test

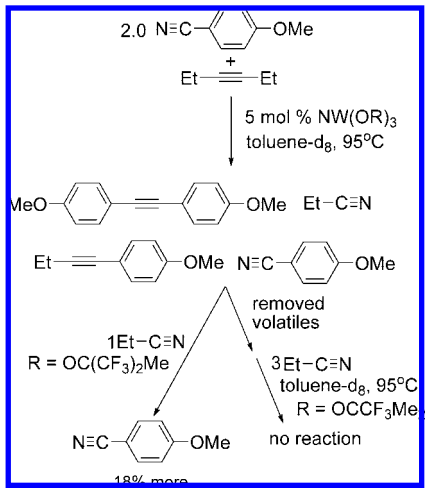

This suggests that the slowest step in NACM catalyzed by **3** is the formation of the propylidyne complex **6** upon reaction of **3** with 3-hexyne. Other alkynes such as ArC≡CEt and ArC≡CAr are even less reactive toward **3**, such that they fail to yield any alkylidyne complex under the conditions employed. This is not the case when **1**-DME is used, however. Formation of the propylidyne complex **5**-DME upon reaction with 3-hexyne is relatively facile, taking place at room temperature. Significantly higher temperatures are needed to complete the NACM cycle, thus indicating that a different step is slow.

Preparation of Alkynes by NACM-ACM or NACM-ACM-AP. By appropriately harnessing the varied reactivity seen based on the quantity of 3-hexyne employed as well as the ability to use AP to drive to symmetrical products, NACM can be used for the preparation of either unsymmetrical or symmetrical alkynes with good selectivity (Scheme 15). For instance, standard NACM conditions with **1**-DME, 3,5-bis(trifluoromethyl)benzonitrile, and 1 equiv of 3-hexyne resulted in the initial formation of 1-(butyn-1-yl)-3,5-bis(trifluoromethyl)benzene in 80% yield. Following removal of volatiles and subjection to AP conditions, the reaction mixture afforded bis(3,5-bis(trifluoromethyl)phenyl-)ethyne in 95% conversion. Similar results were obtained in the reactions of 3,5-dimethylbenzonitrile with 2 equiv of 3-hexyne and 4-cyanostyrene with 1.5 equiv of 3-hexyne (Scheme 15).

Functional Group Tolerance. Tables 5 and 6 summarize an assay of the functional group tolerance of the NACM catalysts **1**-DME and **5**.[1] Several nitriles were tested for functional group compatibility with the catalysts. Those substrates containing alkyl, alkyl halide, vinyl, and many substituted aryl groups resulted in good yields (Table 5). Unfortunately, many Lewis basic substrates including pyridines, most amines, alcohols, and nitroarenes were found to deactivate the catalysts, probably via strong coordination to the W center (Table 6). Table 6 shows that there are at least two different modes of catalyst deactivation. In many cases (Table 6: entries 2, 4, 5, 7, and 9–11), conversion of **1**-DME to **5**-DME occurred stoichiometrically, but **1**-DME was not reformed; therefore, NACM did not occur. Addition of anisonitrile to these reaction mixtures confirmed that the catalyst had been deactivated. In other cases (Table 6: entries 2, 4, 5, 7, and 9–11), **5**-DME was never formed, but the catalyst was likewise deactivated. Some bulky substrates (entries 13 and 14 in Table 6) failed to react but did not destroy the catalyst.

Ketones and aldehydes destroyed the catalysts (Table 6, entries 1 and 2). However, testing of acetals and ketals revealed an intriguing difference between **1**-DME and **3**. The more Lewis acidic **1**-DME was deactivated by these substrates, whereas **3** produced the desired materials (Table 5, entries 10 and 12). A similar departure was noted in reactions of *t*-butyl ester with **1**-DME and **3**: these substrates were tolerated by **3** but not by **1**-DME (Table 5, entry 11). This illustrates that catalyst destruction can be overcome by tuning the Lewis acidity of the tungsten center with the appropriate ancillary ligands. Interestingly, thiophenes, which were previously incompatible with tungsten-based alkyne metathesis catalysts,[5,43] afforded products in excellent yield. Overall, however, the functional group tolerance of NACM catalysts **1**-DME and **3** is more restricted than that of the alkyne metathesis catalyst *t*-BuC≡W(O-*t*-Bu)$_3$[4] as a result of the increased Lewis acidity of the metal center needed for NACM activity.

Solvent Studies. To determine the optimal conditions for NACM, a variety of solvents was investigated at standard conditions of 95 °C using 5 mol % of 6 mM **1**-DME with 2 equiv of anisonitrile and 1 equiv of 3-hexyne (eq 5 and Table 6). Toluene is the optimal solvent for reactions, typically exhibiting the greatest preference for formation of the symmetrical alkyne as well as the most rapid rate of reaction. Reactions performed in benzene and bromobenzene exhibit a decreased alkyne preference and an increase in 3-hexyne polymerization, as indicated by the complete consumption of 3-hexyne with anisonitrile yet remaining. Unlike toluene and bromobenzene, dichloromethane affords similar yields of NACM products. However, no alkyne selectivity was observed. Furthermore, the necessarily lower reaction temperature necessitates a much longer reaction time. Reactions performed in THF proceed extraordinarily slowly. This is most likely a result of coordination of THF to the catalyst. Chloroform and 1,2-dichloroethane afford only moderate yields of alkyne products as a result of relatively rapid catalyst decomposition in these solvents.

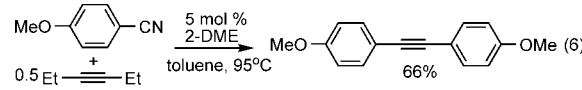

Preparative Application of NACM. To demonstrate the synthetic utility of NACM, we examined the syntheses of some alkynes on a 0.1 mmol scale, as depicted in eqs 6 and 7.[1] We also began to investigate the application of NACM to the synthesis of large molecules. To this end, we completed the synthesis of the cyclic conjugated arylene ethynylene **12** as depicted in eq 8. Compound **12** and other arylene ethynylene macrocycles are of interest for applications in nanomaterials and nanodevices.[44] Use of NACM to prepare **12** streamlines its synthesis by eliminating two steps (one of which requires Pd) and affords the desired product in slightly improved overall yield as compared to the best alternative route.[45] ^{1}H NMR monitoring of the course of the NACM reaction to prepare **12** provided evidence for initial oligomerization prior to macrocycle formation. This situation is frequently observed in ring-closing metathesis reactions.[46,47]

Conclusion

In summary, the tungsten-nitride complexes **1**-DME, **2**, and **3** and their alkylidyne analogues **5**-DME and **6** catalyze the

(43) Furstner, A.; Seidel, G. *J. Organomet. Chem.* **2000**, *606*, 75.

Scheme 15. Procedures for Selective Formation of Symmetrical versus Unsymmetrical Alkynes

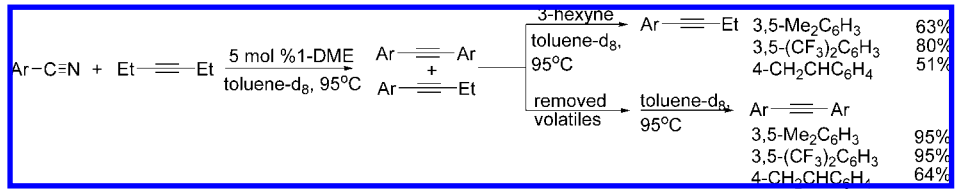

Table 5. Alkyne Formation

Entry	Starting Nitrile	Products (% Yield) Unsymmetrical Alkyne		Symmetrical Alkyne		Time (h)	3-hexyne (equiv)
1	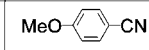	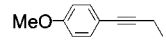	11 18[a]	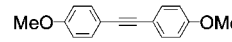	81 61[a]	8 31[a]	1.0 1.0[a]
2	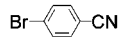	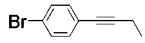	0	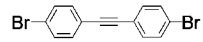	100	15	2.0
3		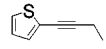	19	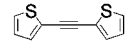	41	11	2.0
4		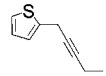	0	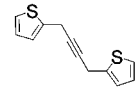	75	22	2.0
5	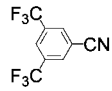	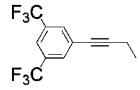	5	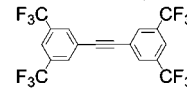	95	25	2.0
6		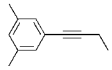	<5	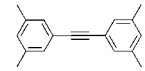	>95	24	2.0
7		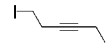	40	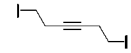	33	6	2.0
8	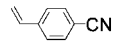	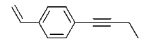	34	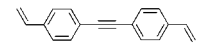	64	13	1.6
9	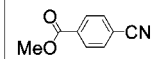	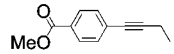	76	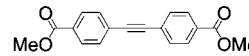	24	24	3.0
10	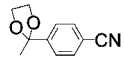	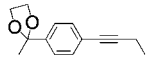	19 58[a]	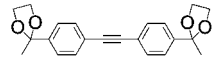	23 12[a]	11 25[a]	1.0 1.0[a]
11	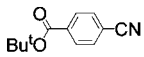	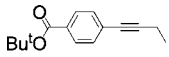	43[a]	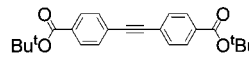	6[a]	20[a]	2.0[a]
12	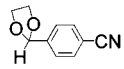	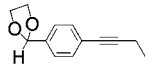	4 25[a]	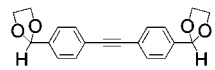	0 0[a]	12 25[a]	1.0 1.0[a]
13	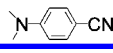	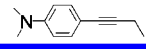	69	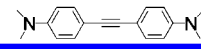	13	18	2.0

95 °C, toluene. [a] catalyst = **3**.

cross-metathesis of internal alkynes with nitriles. DFT calculations on a model system indicate that a [2 + 2] cycloaddition−cycloreversion mechanism is feasible. Variation of ancillary alkoxide ligand identity leads to changes in the NACM catalyst resting state: use of $OC(CF_3)Me_2$ affords nitride **3**, whereas use of $OC(CF_3)_2Me$ favors benzylidyne/alkylidyne species. All steps in NACM are reversible for the reaction of 3-hexyne with anisonitrile catalyzed by **1**-DME, unlike with **3**.

Owing to the rapid ACM equilibrium relative to NACM, use of excess 3-hexyne in NACM reactions favors the formation of unsymmetrical alkynes. Taking advantage of AP, tandem NACM-AM-AP with **1**-DME leads to the formation of the symmetrical alkyne with increased selectivity. Substrate tolerance is catalyst-dependent, with **3** exhibiting the broadest functional group compatibility, although **1**-DME is more active. Many substrates afforded good conversion to alkynes. However, Lewis basic functionalities usually precluded reactivity. Interestingly, **1**-DME displays an unusual tolerance of thiophenes with respect to previously known tungsten-based AM catalysts. We are currently pursuing the development of catalysts that display enhanced activity and functional group tolerance, including non-W-based catalysts.

Experimental Procedures

General Procedures. ^{1}H NMR spectra were recorded at 499.909 MHz on a Varian Inova 500 spectrometer, 399.967 MHz on a Varian Inova 400 spectrometer, or 300.075 MHz on a Varian Inova 300 spectrometer and referenced to the residual protons in C_6D_6 (7.15 ppm), toluene-d_8 (2.09 ppm), CD_2Cl_2 (5.32 ppm), and $CDCl_3$ (7.26 ppm). ^{13}C NMR spectra were recorded at 100.587 MHz on a Varian Inova 400 spectrometer or at 75.465 MHz on a Varian Inova 300 spectrometer and were referenced to naturally abundant ^{13}C nuclei in C_6D_6 (128.00 ppm), $CDCl_3$ (77.16 ppm), or CD_2Cl_2 (54.00 ppm). ^{19}F NMR spectra were recorded at 282.384 MHz on a Varian Inova 300 spectrometer or 376.326 MHz on a Varian Inova

Table 6. Incompatible Substrates[a]

Entry	Starting Nitrile	Cat. Decomp. 1-DME	Cat. Decomp. 5
1	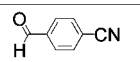	N	Y
2	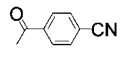	Y	
3	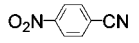	N	Y
4	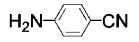	Y	
5	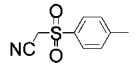	N	Y
6	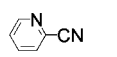	Y	
7	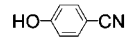	Y	
8	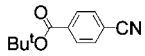	N	Y
9	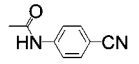	Y	
10	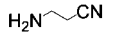	Y	
11	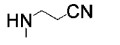	Y	
12	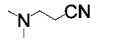	N	Y
13	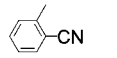	N	N
14	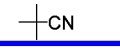	N	N

[a] Y: This catalyst form is deactivated.

400 spectrometer and were referenced to an external standard of $CFCl_3$ in $CDCl_3$ (0.00 ppm). MALDI-TOF data were collected on a Micromass TofSpec-2E matrix-assisted laser-desorption time-of-flight mass [33]spectrometer.

Materials and Methods. All reactions were performed in an atmosphere of dinitrogen, either in a nitrogen-filled MBRAUN Labmaster 130 glovebox or by using standard air-free techniques.[48] All solvents used were dried and deoxygenated by the method of Grubbs et al.[49] $[N{\equiv}WCl_3]_4{\cdot}1.1DCE$,[29] $LiOC(CF_3)_2Me$,[50] 1-(4-methoxyphenyl)-1-butyne,[11] $W_2(OCMe_2CF_3)_6$,[30] $[Li(dme)_2][NW(OC(CF_3)_2Me)_4]$ (**2**), $[NW(OCMe_2CF_3)_3]_3$ (**3**),[1] 1-(4-trifluoromethylphenyl)-1-butyne,[11] bis(4-trifluoromethylphenyl)acetylene,[51] and bis(4-methoxyphenyl)acetylene[1] were prepared according to literature procedures. $LiOCMe_2CF_3$ was prepared in a manner analogous to that used for the preparation of $LiOC(CF_3)_2Me$. NMR solvents were obtained from Cambridge Isotope Laboratories and were dried over 4 Å molecular sieves for at least 24 h. DME was obtained anhydrous from Aldrich and was further dried over 4 Å molecular sieves for 48 h and run through a plug of alumina before use. 1-Bromotetradecane, sodium hydride (60% in mineral oil), bromobenzene, copper(I) cyanide, and 3-hexyne were obtained from Acros. Propionitrile and 3,6-dibromocarbazole were obtained from Aldrich. Propionitrile and 3-hexyne were dried for 24 h using 4 Å molecular sieves. DMF was dried for 1 month over 4 Å molecular sieves. All other reagents were used as received.

Catalyst Syntheses. $NW(OC(CF_3)_2Me)_3(DME)$ (1-DME). $[N{\equiv}WCl_3]_4{\cdot}1.1DCE$ (4.00 g, 3.02 mmol) and $LiOC(CF_3)_2Me$ (6.81 g, 36.2 mmol, 12.0 equiv) were slurried in toluene (40 mL) in a bomb flask. THF (982 μL, 12.1 mmol, 4 equiv) was added via syringe, and the bomb flask was sealed. The reaction mixture was heated with stirring for 19.5 h at 65 °C. The reaction mixture was heated to nearly boiling and filtered through Celite. The Celite was washed with hot toluene (40 mL). The volatiles were removed in vacuo from the filtrate. The resulting residue was taken up in Et_2O (12 mL) and DME (1.25 mL, 12.07 mmol, 4 equiv). Pentane (8 mL) was added, and the solution was cooled to −35 °C. Complex **1** was collected as yellow crystals via filtration (6.01 g, 7.23 mmol, 60% yield). Characterization data agreed with the literature.[1]

$[NW(OCMe_2CF_3)_3]_3$ (3). $W_2(OCMe_2CF_3)_6$ (10.0 mg, 0.00885 mmol) was dissolved in toluene-d_8 (0.5 mL). Propionitrile (1.2 μL, 0.0173 mmol, 2.0 equiv) was introduced via syringe, and the resulting reaction mixture was heated at 95 °C for 18.5 h. At this point, ^{1}H NMR and ^{19}F NMR indicated complete conversion to **3**.[23]

$CH_3CH_2C{\equiv}W(OC(CF_3)_2Me)_3(DME)$ (5-DME). **1**-DME (450 mg, 0.541 mmol) was dissolved in toluene (10 mL), and the solution was transferred to a bomb flask. To this solution 3-hexyne (61.5 μL, 0.541 mmol, 1 equiv) was added via syringe. The bomb flask was sealed and heated at 95 °C for 16 h. ^{1}H NMR spectroscopy indicated incomplete conversion to the alkylidyne. Additional 3-hexyne (20.0 μL, 0.176 mmol, 0.325 equiv) was syringed into the reaction mixture. This was then heated at 95 °C for 2 h. The resulting mixture was then filtered through Celite to remove poly-3-hexyne. The volatiles were removed in vacuo from the filtrate. The red residue was then taken up in 5 mL of pentane and cooled to −35 °C. A red powder, **5**, was collected via filtration (242.8 mg, 0.283 mmol, 52%). Characterization data agreed with the literature.[6]

$CH_3CH_2C{\equiv}W(OCMe_2CF_3)_3$ (6). $W_2(OCMe_2CF_3)_6$ (570.4 mg, 0.505 mmol) was dissolved in toluene (10 mL). 3-Hexyne (68.8 μL, 0.605 mmol, 1.2 equiv) was added via syringe, and the reaction mixture was stirred for 1 h. The volatiles were removed in vacuo, and the resulting residue was taken up in 10 mL of pentane. The pentane solution was filtered, and the filtrate was reduced in volume to 2 mL. The resulting solution was cooled to −35 °C. A powder of **6** was collected via filtration (528.2 mg, 0.871 mmol, 86%). ^{1}H NMR (300 MHz, tol-d_8): δ 3.40 (q, 2H, ≡CCH_2CH$_3$, J = 8.2 Hz), 1.31 (d, 2H, ArH, J = 8.4 Hz), 1.65 (s, 18H, OC(CH_3)$_2$CF$_3$). ^{19}F NMR (400 MHz, C_6D_6): −82.59(OC(CH$_3$)$_2$CF_3). ^{13}C{^{1}H} NMR (400 MHz, CD_2Cl_2): δ 274.18 (t, W≡C, J_{W-C} = 148.1 Hz), 127.39 (q, OC(CH$_3$)$_2$$CF_3$, J_{C-F} = 284.0 Hz), 82.29 (q, OCCF$_3$(CH$_3$)$_2$, J_{C-F} = 28.8 Hz), 40.71 (s, CCH$_2$CH$_3$), 25.62 (s, OC(CH_3)$_2$CF$_3$), 16.89 (s, CCH$_2$$CH_3$).[30]

4-MeO(C_6H_4)C≡W(OC(CF_3)$_2$Me)$_3$(DME) (7-DME). **1**-DME (200 mg, 0.241 mmol) and 1-(4-methoxyphenyl)-1-butyne (38.8 mg, 0.241 mmol, 1 equiv) were slurried in toluene-d_8 (1 mL) in a J. Young tube. This mixture was heated at 95 °C for 2.5 h. The volatiles were removed in vacuo. The resulting residue was reconstituted in toluene-d_8 (1 mL) and heated at 95 °C for 2 h. The volatiles were removed in vacuo. The remaining material was dissolved in a total of 4 mL of 1:1 Et_2O/pentane and cooled to

(44) Naddo, T.; Che, Y. K.; Zhang, W.; Balakrishnan, K.; Yang, X. M.; Yen, M.; Zhao, J. C.; Moore, J. S.; Zang, L. *J. Am. Chem. Soc.* **2007**, *129*, 6978.
(45) Zhang, W.; Moore, J. S. *J. Am. Chem. Soc.* **2004**, *126*, 12796.
(46) Zhang, W.; Moore, J. S. *J. Am. Chem. Soc.* **2005**, *127*, 11863.
(47) Conrad, J. C.; Eelman, M. D.; Silva, J. A. D.; Monfette, S.; Parnas, H. H.; Snelgrove, J. L.; Fogg, D. E. *J. Am. Chem. Soc.* **2007**, *129*, 1024.
(48) Shriver, D. G.; Sailor, M. J. *The Manipulations of Air-Sensitive Compounds*, 2nd ed.; Wiley-Interscience: New York, 1986.
(49) Pangborn, A. B.; Giardello, M. A.; Grubbs, R. H.; Rosen, R. K.; Timmers, F. J. *Organometallics* **1996**, *15*, 1518.
(50) delaMata, F. J.; Grubbs, R. H. *Organometallics* **1996**, *15*, 577.
(51) Shirakawa, E.; Kitabata, T.; Otsuka, H.; Tsuchimoto, T. *Tetrahedron* **2005**, *61*, 9878.

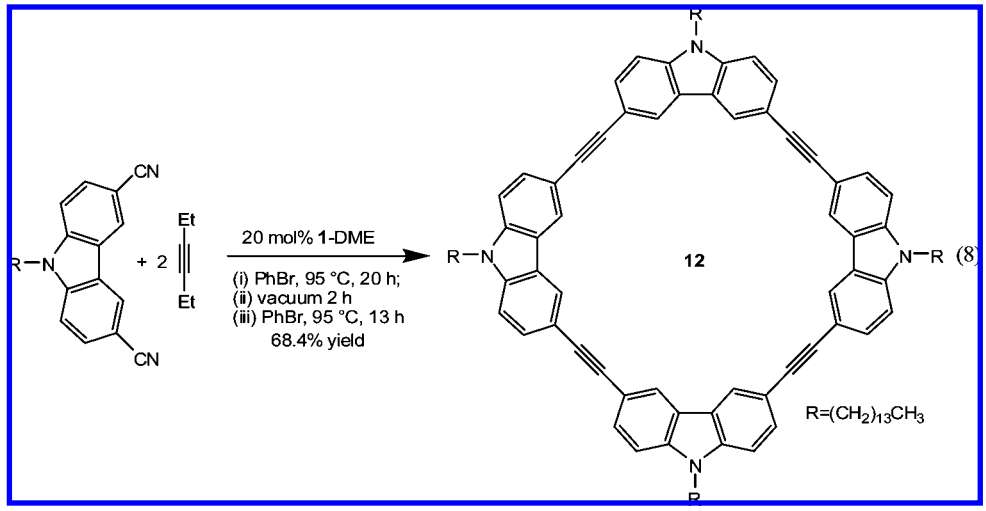

−35 °C. The product (**7**), a deep red−orange powder, was collected via filtration (124.2 mg, 0.133 mmol, 67%). ^{1}H NMR (500 MHz, C_6D_6): δ 6.81 (d, 2H, ArH, J = 6.8 Hz), 6.71 (d, 2H, ArH, J = 6.8 Hz), 3.65 (br s, 3H, DME), 3.25 (s, 3H, OCH_3), 3.20 (br s, 4H, DME), 2.92 (br s, 3H, DME), 1.88 (s, 9H, OC$(CF_3)_2CH_3$). ^{1}H NMR (300 MHz, toluene-d_8, −20 °C): δ 6.80 (d, 2H, ArH, J = 9.0 Hz), 6.65 (d, 2H, ArH, J = 9.0 Hz), 3.65 (s, 3H, DME), 3.21 (s, 3H, OCH_3), 3.10 (s, 3H, DME), 3.07 (t, 2H, DME, J = 4.3 Hz), 2.86 (t, 2H, DME, J = 4.3 Hz), 1.89 (s, 9H, OC$(CF_3)_2CH_3$). ^{19}F NMR (400 MHz, CD_2Cl_2): δ −77.05 (s). ^{13}C{^{1}H} NMR (400 MHz, CD_2Cl_2): δ 278.26 (s) (W≡*C*), 160.05 (s) (Ar), 137.84 (s) (Ar), 135.47 (s) (Ar), 124.7 (q) (OC(*C*$F_3)_2CH_3$, J_{C-F} = 289.00 Hz), 112.76 (s) (Ar), 83.11 (m) (O*C*$(CF_3)_2CH_3$), 75.34 (s) (DME), 73.00 (s) (DME), 70.60 (s) (DME), 59.50 (s) (DME), 55.64 (s) (O*C*H_3), 18.97 (s) (OC$(CF_3)_2$*C*H_3). Anal. calcd for $WO_6C_{24}H_{26}F_{18}$: C, 30.79; H, 2.80. Found: C, 30.97; H, 2.96.

4-F_3C(C_6H_4)C≡W(OC$(CF_3)_2Me)_3$(DME) (8-DME). **1**-DME (250 mg, 0.301 mmol) and 1-(4-trifluoromethylphenyl)-1-butyne (59.9 mg, 0.301 mmol, 1 equiv) were slurried in toluene-d_8 (1 mL) in a J. Young tube. The reaction mixture was heated at 95 °C for 12 h. The volatiles were removed in vacuo. The resulting residue was dissolved in 5 mL of pentane and cooled to −35 °C. The product, a deep yellow powder, was collected via filtration (95.0 mg, 0.0975 mmol, 32%). A second crop of 71.2 mg was collected to give a total yield of 57% (0.171 mmol). ^{1}H NMR (500 MHz, C_6D_6): δ 7.33 (d, 2H, ArH, J = 8.2 Hz), 6.70 (d, 2H, ArH, J = 8.2 Hz), 3.57 (br s, 3H, DME), 3.78 (br s, 2H, DME), 3.44 (br s, 3H, DME), 1.83 (s, 9H, OC$(CF_3)_2CH_3$). ^{1}H NMR (300 MHz, toluene-d_8, −20 °C): δ 7.25 (d, 2H, ArH, J = 8.1 Hz), 6.68 (d, 2H, ArH, J = 8.1 Hz), 3.56 (s, 3H, DME), 3.07 (s, 3H, DME), 3.04 (t, 2H, DME, J = 4.3 Hz), 2.82 (t, 2H, DME, J = 4.3 Hz), 1.89 (s, 9H, OC$(CF_3)_2CH_3$).^{19} F NMR (400 MHz, CD_2Cl_2): δ −63.21 (s, CF_3) −77.61 (s, OC$(CF_3)_2CH_3$). ^{13}C{^{1}H} NMR (400 MHz, CD_2Cl_2): δ 276.41 (s, W≡*C*), 146.44 (s, Ar), 134.13 (s, Ar), 129.13 (q, Ar, J_{C-F} = 65.3 Hz), 124.50 (q, OC(*C*$F_3)_2CH_3$, J_{C-F} = 289.0 Hz), 123.86 (q, Ar, J_{C-F} = 272.1 Hz), 124.66 (q, Ar, J_{C-F} = 4.4 Hz), 83.28 (m, O*C*$(CF_3)_2CH_3$), 75.71 (s, DME), 73.55 (s, DME), 69.96 (s, DME), 59.94 (s, DME), 18.87 (s, OC$(CF_3)_2$*C*H_3). Anal. calcd for $WO_5C_{24}H_{23}F_{21}$: C, 29.59; H, 2.38. Found: C, 29.38; H, 2.19.

MeO(C_6H_4)C≡W$(OCMe_2CF_3)_3$ (9). Complex **6** (200 mg, 0.330 mmol) was dissolved in toluene (5 mL). To this solution, solid bis(4-methoxyphenyl)acetylene (39.3 mg, 0.165 mmol) was added. The solution was diluted with toluene (5 mL). The reaction mixture was stirred for 1 h. Then the volatiles were removed in vacuo. The resulting mixture was dissolved in pentane (15 mL) and filtered. The volume of the filtrate was reduced to 6 mL, and the solution was cooled to −35 °C. Deep yellow−orange crystals of **9** were isolated via filtration and washed with 2 mL of cold pentane (188 mg, 0.274 mmol, 83% yield). ^{1}H NMR (400 MHz, CD_2Cl_2): δ 7.00 (d, 2H, ArH, J = 8.8 Hz), 6.87 (d, 2H, ArH, J = 8.6 Hz), 3.79 (s, 3H, OCH_3), 1.64 (s, 18H, OC$(CH_3)_2CF_3$). ^{19}F NMR (400 MHz, CD_2Cl_2): δ −83.17 (s, OC$(CH_3)_2CF_3$). ^{13}C{^{1}H} NMR (400 MHz, CD_2Cl_2): δ 264.99 (s, W≡*C*), 158.34 (s, Ar), 138.94 (s, Ar), 132.83 (s, Ar), 125.94 (q, OC$(CH_3)_2CF_3$, J_{C-F} = 284.4 Hz), 112.23 (s, Ar), 81.83 (q, O*C*$F_3(CH_3)_2$, J_{C-F} = 28.8 Hz), 54.76 (s, OMe), 24.36 (s, OC$(CH_3)_2CF_3$). Anal. calcd for $WO_4C_{20}H_{25}F_9$: C, 35.11; H, 3.68. Found: C, 34.86; H, 3.43.

4-F_3C(C_6H_4)C≡W$(OCMe_2CF_3)_3$) (10). Complex **6** (200 mg, 0.330 mmol) was dissolved in toluene (5 mL). Then, bis(4-trifluoromethylphenyl)acetylene (51.8 mg, 0.165 mmol, 2.0 equiv) was dissolved in toluene (5 mL) and added to the solution of **6**. The reaction mixture was stirred for 1 h. The volatiles were removed in vacuo. The resulting mixture was dissolved in pentane (10 mL) and filtered. The volume of the filtrate was reduced to 3 mL, and the solution was cooled to −35 °C. Light yellow feathers of **10** were collected via filtration and washed with 2 mL of cold pentane (175 mg, 0.242 mmol, 73% yield). ^{1}H NMR (400 MHz, CD_2Cl_2): δ 7.62 (d, 2H, ArH, J = 8.2 Hz), 7.13 (d, 2H, ArH, J = 8.4 Hz), 1.65 (s, 18H, OC$(CH_3)_2CF_3$). ^{19}F NMR (400 MHz, CD_2Cl_2): δ −83.18 (s, 9F, OC$(CH_3)_2CF_3$), −62.99 (s, 3F, ArCF_3). ^{13}C{^{1}H} NMR (400 MHz, CD_2Cl_2): δ 265.11 (t, W≡*C*, J_{C-W} = 152.0 Hz), 148.95 (s, Ar), 133.06 (s, Ar), 127.16 (q, OC$(CH_3)_2$*C*F_3, J_{C-F} = 268.2 Hz), 124.56 (q, Ar, J_{C-F} = 271.4 Hz), 125.32 (q, Ar, J_{C-F} = 4.0 Hz), 83.74 (q, O*C*$F_3(CH_3)_2$, J_{C-F} = 29.2 Hz), 25.71 (s, OC$(CH_3)_2CF_3$). Anal. calcd for $WO_3C_{20}H_{22}F_{12}$: C, 33.26; H, 3.07. Found: C, 33.15; H, 3.13.

O=W$(OCMe_2CF_3)_4$ (11). Complex **3** (500 mg, 0.863 mmol) was dissolved in toluene (10 mL) in a bomb flask. 3-Hexyne (294 μL, 2.59 mmol, 3 equiv) was added via syringe to the solution, and the bomb flask was sealed and heated at 95 °C for 2 days. The reaction mixture was filtered through Celite with Et_2O (40 mL). The filtrate was dried in vacuo and taken up in pentane (20 mL). The mixture was again filtered, and the resulting filtrate was reduced to 5 mL and cooled to −35 °C. Deep orange crystals of **11** were collected via filtration and washed with 3 mL of cold pentane (111.6 mg, 0.158 mmol, 24% yield). ^{1}H NMR (400 MHz, tol-d_8): δ 1.43 (s, OC$(CH_3)_2CF_3$). ^{19}F NMR (400 MHz, tol-d_8): δ −81.4 (s, OC$(CH_3)_2CF_3$). ^{13}C{^{1}H} NMR (400 MHz, C_6D_6): δ 127.67 (q, OC(*C*$F_3)_2CH_3$, J_{C-F} = 285.4 Hz), 84.60 (q, CAr, J_{C-F} = 29.9 Hz), 22.10 (s, OC$(CF_3)_2$*C*H_3). Anal. calcd for $WO_5C_{16}H_{24}F_{12}$: C, 27.14; H, 3.42. Found: C, 27.13; H, 3.32.

(Et_3C_3)W$(OCMe_2CF_3)_3$ (12). Complex **6** (160.0 mg, 0.264 mmol) was dissolved in CD_2Cl_2 (500 μL). 3-Hexyne (33.0 μL, 0.290 mmol, 1.1 equiv) was introduced to the solution via syringe. The resulting ^{1}H NMR spectrum was observed at −60 °C. The complete removal of volatiles resulted in conversion to **6**. ^{1}H NMR (300 MHz, tol-d_8, −60 °C): δ 3.56 (q, 4H, $C_\alpha CH_2CH_3$, J = 7.0 Hz), 2.62 (q, 2H, $C_\beta CH_2CH_3$, J = 7.0 Hz), 1.81 (s, 6H, OC$(CH_3)_2CF_3$), 1.37 (t, 6H, $C_\alpha CH_2CH_3$, J = 7.0 Hz), 1.65 (s, 18H, OC$(CH_3)_2CF_3$), 0.95 (s, 18H, OC$(CH_3)_2CF_3$), 0.76 (t, 3H, $C_\beta CH_2CH_3$, J = 7.0 Hz).

^{19}F NMR (300 MHz, tol-d_8, −60 °C): −81.30 (s, 6F, OC(CH$_3$)$_2$CF_3 ax), −81.55 (s, 3F, OC(CH$_3$)$_2$CF_3 eq). ^{13}C{^{1}H} NMR (300 MHz, CD_2Cl_2, −60 °C): δ 238.19 (t, W−C_α, J_{W-C} = 61.7 Hz), 130.47 (s, W−C_β), 127.92 (q, OC(CH$_3$)$_2$CF$_3$ eq, J_{C-F} = 286.2 Hz), 27.60 (q, OC(CH$_3$)$_2$CF$_3$ ax, J_{C-F} = 287.4 Hz), 81.25 (q, OCCF$_3$(CH$_3$)$_2$ eq, J_{C-F} = 28.5 Hz), 76.34 (q, OCCF$_3$(CH$_3$)$_2$ ax, J_{C-F} = 27.3 Hz), 29.97 (s, OC(CH$_3$)$_2$CF$_3$ eq), 25.08 (s, C$_\alpha$CH$_2$CH$_3$), 25.62 (s, OC(CH$_3$)$_2$CF$_3$), 20.02 (s, C$_\beta$CH$_2$CH$_3$), 14.26 (s, CH$_3$), 12.30 (s, CH$_3$).

Substrate Syntheses. 3,6-Dibromo-9-tetradecyl-9*H*-carbazole. In a glovebox, a solution of THF/DMF (30 mL/10 mL) was placed in a 250 mL three-necked flask fitted with a gas adapter, rubber septum, and a solid addition funnel containing NaH (60% in mineral oil, 0.48 g, 12.0 mmol, 1.6 equiv). Under N_2 flow on a Schlenk line, 3,6-dibromocarbazole (2.51 g, 7.72 mmol, 1.01 equiv) was added to the flask, then 1-bromotetradecane (2.28 mL, 7.66 mmol) was added via syringe. The resulting solution was cooled to 0 °C, and then the NaH was added with stirring. The solution was allowed to warm overnight with stirring, and then the volatiles were removed in vacuo. The remaining mixture was quenched with 1 M HCl (50 mL). The product was extracted with $CHCl_3$ (75 mL), and the organic layer was washed with H_2O (3 × 50 mL). The solvent was removed, and the resulting powder was washed with cold pentane (2 × 20 mL) and dried in vacuo, yielding white needles (3.45 g, 6.62 mmol, 86.4%). ^{1}H NMR (300 MHz, CD_2Cl_2): δ 8.16 (s, 2H, Ar*H*), 7.57 (d, 2H, Ar*H*, $^3J_{H-H}$ = 8.7 Hz), 7.33 (d, 2H, Ar*H*, $^3J_{H-H}$ = 8.7 Hz), 4.26 (t, 2H, NC*H*$_2$, $^3J_{H-H}$ = 7.5 Hz), 1.83 (m, 2H, NCH$_2$C*H*2), 1.23−1.53 (m, 22H, (C*H*$_2$)$_{11}$), 0.88 (t, 3H, C*H*$_3$, $^3J_{H-H}$ = 6.6 Hz). ^{13}C{^{1}H} NMR ($CDCl_3$): δ 139.35, 129.07, 123.50, 123.31, 112.02, 110.46, 43.41, 32.08, 29.83, 29.80, 29.78, 29.73, 29.68, 29.60, 29.52, 29.47, 28.96, 27.34, 22.85, 14.29. Anal. calcd for $C_{26}H_{35}NBr_2$: C, 59.90; H, 6.77; N, 2.69. Found: C, 60.06; H, 6.45; N, 2.65.

9-Tetradecyl-9*H*-carbazole-3,6-dicarbonitrile. In a glovebox, dry DMF (30 mL) was measured into a 100 mL two-necked flask equipped with a rubber septum and gas adapter. Under N_2 flow on a Schlenk line, 3,6-dibromo-9-tetradecyl-9*H*-carbazole (3.17 g, 6.08 mmol) and copper(I) cyanide (2.00 g, 22.3 mmol) were added to the flask. A reflux condensor was fitted under N_2 flow, and the solution was heated to reflux with stirring for 26 h. The solution was cooled to room temperature, and then concentrated NH_4OH (20 mL) was added. After stirring for 10 min, the mixture was extracted with CH_2Cl_2 (2 × 50 mL). The combined organics were washed with H_2O (2 × 50 mL) and brine (50 mL), and then filtered through a plug of silica to remove solid impurities. The silica plug was washed with CH_2Cl_2 until the filtrate ran colorless. The combined filtrate was concentrated to dryness. The resulting powder was washed with acetone, then dried in vacuo, yielding a brown powder (1.35 g, 3.26 mmol, 53.6%). ^{1}H NMR (300 MHz, $CDCl_3$): δ 8.41 (s, 2H, Ar*H*), 7.79 (d, 2H, Ar*H*, $^3J_{H-H}$ = 8.4 Hz), 7.52 (d, 2H, Ar*H*, $^3J_{H-H}$ = 8.4 Hz), 4.35 (t, 2H, NC*H*$_2$, $^3J_{H-H}$ = 6.9 Hz), 1.83−1.90 (m, 2H, -NCH$_2$C*H*$_2$), 1.22−1.33 (m, 22H, (C*H*$_2$)$_{11}$), 0.87 (t, 3H, C*H*$_3$, $^3J_{H-H}$ = 6.6 Hz). ^{13}C{^{1}H} NMR ($CDCl_3$): δ 142.84, 130.40, 125.81, 122.24, 119.92, 110.33, 103.57, 43.90, 32.04, 29.78, 29.76, 29.74, 29.69, 29.60, 29.54, 29.48, 29.39, 28.98, 27.31, 22.81, 14.25. Anal. calcd for $C_{28}H_{35}N_3$: C, 81.31; H, 8.53; N, 10.16. Found: C, 80.87; H, 8.41; N, 10.01.

Tetramer (12). In a glovebox, **1**-DME (93.4 mg, 0.112 mmol) and 9-tetradecyl-9*H*-carbazole-3,6-dicarbonitrile (250.5 mg, 0.606 mmol) were weighed into a bomb flask. Bromobenzene (37 mL) and 3-hexyne (0.14 mL, 1.23 mmol) were added, and then the bomb flask was sealed and placed in a 95 °C oil bath. After 20 h, the solution was cooled and a vacuum was pulled for 2 h to remove volatile products. The bomb flask was sealed and heated for an additional 13 h. The solution was cooled and washed through a plug of silica with $CHCl_3$ (150 mL). The filtrate was concentrated to dryness, then precipitated from $CHCl_3$/pentane at −20 °C. The mixture was filtered, and the precipitate was dried in vacuo to give an off-white powder (161.1 mg, 0.104 mmol, 68.4%). ^{1}H NMR matched the literature values.[45,52] MALDI-TOF [m/z]$^+$: 1542.1 ($C_{112}H_{140}N_4$)

Crystal Structure Determinations. 1-DME. Colorless needles of **1**-DME were grown from a pentane/diethyl ether solution at −35 °C. A crystal of dimensions 0.44 mm × 0.42 mm × 0.16 mm was mounted on a standard Bruker SMART 1K CCD-based X-ray diffractometer equipped with a LT-2 low-temperature device and normal focus Mo-target X-ray tube (λ = 0.71073 A) operated at 2000 W (50 kV, 40 mA). The X-ray intensities were measured at 108(2) K; the detector was placed at a distance of 4.969 cm from the crystal. A total of 3000 frames was collected with a scan width of 0.5° in ω and φ with an exposure time of 20 s/frame. The integration of the data yielded a total of 111 329 reflections to a maximum 2θ value of 56.82°, of which 12 760 were independent and 12 059 were greater than 2σ(I). The final cell constants (Table 1) were based on the *xyz* centroids of 8931 reflections above 10σ(I). Analysis of data showed negligible decay during data collection; the data were processed with SADABS and corrected for absorption. The compound crystallized as a pseudo-merohedral twin with twin law (100, 0−10, 00−1) and twin scale factor 0.3732(8). The structure was solved and refined with the Bruker SHELXTL (version 6.12) software package, using the space group $P2(1)/c$ with Z = 8 for the formula $C_{16}H_{19}F_{18}NO_5W$. All non-hydrogen atoms were refined anisotropically with the hydrogen atoms placed in idealized positions. Full matrix least-squares refinement based on F^2 converged at R1 = 0.0533 and wR2 = 0.1384 [based on I > 2σ(I)] and R1 = 0.0569 and wR2 = 0.1411 for all data.

Complex 2. Colorless needles of **2** were grown from a toluene/pentane solution at −35 °C. A crystal of dimensions 0.46 mm × 0.26 mm × 0.22 mm was mounted on a Bruker SMART-1K CCD-based X-ray diffractometer equipped with a low-temperature device and fine focus Mo-target X-ray tube (λ = 0.71073 A) operated at 1500 W (50 kV, 40 mA). The X-ray intensities were measured at 108(2) K; the detector was placed at a distance 4.912 cm from the crystal. A total of 2342 frames were collected with a scan width of 0.5° in ω and 0.45° in φ with an exposure time of 20 s/frame. The integration of the data yielded a total of 298 848 reflections to a maximum 2θ value of 56.64° of which 37 755 were independent and 34 774 were greater than 2σ(I). The final cell constants (Table 1) were based on the *xyz* centroids of 9771 reflections above 10σ(I). Analysis of data showed negligible decay during data collection; the data were processed with SADABS and corrected for absorption. The structure was solved and refined with the Bruker SHELXTL (version 6.12) software package, using the space group $P2(1)/c$ with Z = 16 for the formula $C_{24}H_{32}NLiO_8F_{24}W$. There are four crystallographically independent complexes in the asymmetric unit. The structure is a pseudo-orthorhombic twin with twin law (100, −100, 00−1). The refined twin fraction is 0.3915(2). All non-hydrogen atoms were refined anisotropically with the hydrogen atoms placed in idealized positions. The dimethoxyethane ligands are disordered on one complex. Full matrix least-squares refinement based on F^2 converged at R1 = 0.0236 and wR2 = 0.0486 [based on I > 2σ(I)], and R1 = 0.0292 and wR2 = 0.0504 for all data.

Acknowledgment. This material is based upon work supported by the National Science Foundation under Grant CHE-0449459. A.M.G. thanks the University of Michigan Chemistry Department for a Robert W. Parry Inorganic Chemistry Graduate Fellowship. J.B.G. thanks the National Science Foundation for a Graduate Research Fellowship.

(52) Cho, H. M.; Weissman, H.; Wilson, S. R.; Moore, J. S. *J. Am. Chem. Soc.* **2006**, *128*, 14742.

Supporting Information Available: Full crystallographic details for **1**-DME and **2**. Experimental data for reversibility of NACM and ACM, direct monitoring of catalytic reaction progress, optimization studies, influence of AP studies, catalyst comparison studies, functional group tolerance. Coordinates for all atoms, bond lengths and angles of optimized structures in DFT calculations. This material is available free of charge via the Internet at http://pubs.acs.org.

JA800020W